CHEMISTRY
A EUROPEAN JOURNAL

DOI: 10.1002/chem.200700324

Lanthanide Class of a Trinuclear Enantiopure Helical Architecture Containing Chiral Ligands: Synthesis, Structure, and Properties

Marco Lama,[a] Olimpia Mamula,*[a] Gregg S. Kottas,[b] Fabio Rizzo,[b] Luisa De Cola,[b] Asao Nakamura,[c] Reiko Kuroda,[d] and Helen Stoeckli-Evans[e]

Abstract: The pinene-bipyridine carboxylic derivatives (+)- and (−)-HL, designed to form configurationally stable lanthanide complexes, proved their effectiveness as chiral building blocks for the synthesis of lanthanide-containing superstructures. Indeed a self-assembly process takes place with complete diastereoselectivity between the enantiomerically pure ligand L^- and Ln^{III} ions (La, Pr, Nd, Sm, Eu, Gd, Tb, Dy, Ho, Er), thus leading to the quantitative formation of a trinuclear supramolecular architecture with the general formula $[Ln_3(L)_6(\mu_3\text{-}OH)(H_2O)_3](ClO_4)_2$ (abbreviated as tris(Ln[L]$_2$)). This class of C_3-symmetrical compounds was structurally characterized in the solid state and solution. Electrospray (ES) mass spectrometric and ^{1}H NMR spectroscopic analyses indicated that the trinuclear species are maintained in solution (CH_2Cl_2) and are stable in the investigated concentration range (10^{-2}–10^{-6} M). The photophysical properties of the ligand HL and its tris(Ln[L]$_2$) complexes were studied at room temperature and 77 K, thus demonstrating that the metal-centered luminescence is well sensitized both for the visible and near-IR emitters. The chiroptical properties of tris(Ln[L]$_2$) complexes were investigated by means of circular dichroism (CD) and circularly polarized luminescence (CPL). A high CD activity is displayed in the region of π–π* transitions of bipyridine. CPL spectra of tris(Eu[(+)-L]$_2$) and tris(Tb[(+)-L]$_2$) present large dissymmetry factors g_{em} for the sensitive transitions of Eu^{III} ($^5D_0 \rightarrow {}^7F_1$, $g_{em} = -0.088$) and Tb^{III} ($^5D_4 \rightarrow {}^7F_5$, $g_{em} = -0.0806$). The self-recognition capabilities of the system were tested in the presence of artificial enantiomeric mixtures of the ligand. ^{1}H NMR spectra identical to those of the enantiomerically pure complexes and investigations by CD spectroscopic analysis reveal an almost complete chiral self-recognition in the self-assembly process, thus leading to mixtures of homochiral trinuclear structures.

Keywords: chiral recognition · chirality · helical structures · lanthanides · self-assembly

Introduction

Due to their interesting magnetic properties, chiral lanthanides complexes have been used for decades as chiral shift reagents. The role of the enantiopure ligand in this case is to provide the chiral environment necessary to render the enantiotopic nuclei of the substrates diastereotopic. The absolute configuration of a wide range of compounds[1,2] from simple organic molecules or metabolites to proteins has been determined in this way. Lanthanide complexes are also

[a] Dr. M. Lama, Dr. O. Mamula[+]
Institut des Sciences et Ingénierie Chimiques
Ecole Polytechnique Fédérale de Lausanne
BCH 1403, 1015 Lausanne (Switzerland)
Fax: (+41) 21-693-9815
E-mail: olimpia.mamula.steiner@gmail.com

[b] Dr. G. S. Kottas, F. Rizzo, Prof. L. De Cola
Physikalisches Institut
Westfälische Wilhelms-Universität Münster
Mendelstrasse 7, 48149 Münster (Germany)

[c] Prof. A. Nakamura
Shibaura Institute of Technology
Fukasaku, Minuma-ku, Saitama-shi
Saitama 337–8570 (Japan)

[d] Prof. R. Kuroda
ERATO-SORST Kuroda Chiromorphology Team
Japan Science and Technology Agency, Komaba
Meguro-ku, Tokyo, 153–0041 (Japan)

[e] Prof. H. Stoeckli-Evans
Institut de Microtechnologie
Université de Neuchâtel
Rue Emile-Argand 11, 2009 Neuchâtel (Switzerland)

[+] Present address: Champ des Fontaines 29
1700 Fribourg (Switzerland)

Supporting information for this article is available on the WWW under http://www.chemeurj.org/ or from the author.

used as Lewis acid catalysts for carbon–carbon bond formation (for example, the Strecker reaction)[3,4] or ligand substitutions. When chiral ligands, such as binaphthol, are coordinated to a metal center, these reactions are highly stereoselective.[5,6] However, the intrinsic chirality of all of these compounds has been largely neglected for a long time. The development of appropriate techniques for the study of chiral luminescent lanthanide complexes, including circularly polarized luminescence (CPL) in the 1980s, provided an impulse for research in this field. The enantiopure ligands most frequently used were amino acids, carboxylic acids, aminopolycarboxylic acids, and camphor-derived β-diketonates.[7,8] In addition, it has been shown that by adding a chiral probe, an induced shift is obtained in racemic D_3 complexes containing tridentate achiral ligands (i.e., dipicolinic and oxydiacetic acids).[9,10] This chiral induction, which operates at the chiral metal center, is called the Pfeiffer effect and is attributed to an outer-sphere chiral discrimination phenomenon.[11] If the chiral probe is an enantiopure quencher (e.g., metalloproteins, vitamin B_{12}, etc.), then the enantioselective quenching of lanthanide luminescence can be studied.[12]

Recently, the interesting potential of coordinatively unsaturated chiral Ln^{III} complexes for the molecular-recognition phenomena of chiral[13] and ionic[14–16] substrates has attracted much attention. Chiroptical studies have also shown substantial alterations in the coordination sphere induced by the nature of the solvent, pH value, chelation, and conformational changes in the ligands. As an example, complexes with archetypal bidentate enantiopure β-diketonate ligands show that the degree of chirality sensed by the central Ln^{III} cation changes when an achiral amine is used as the solvent.[17] This labile behavior prevents, in most cases, the use of successful techniques applied for obtaining enantiomerically pure complexes with transition metals, that is, diastereoisomeric resolution and/or diastereoselective synthesis through chiral ligands. Consequently, reports of the synthesis of enantiopure, configurationally stable Ln^{III} complexes are scarce and almost exclusively concern mononuclear structures.[18–21] Only two examples of enantiopure, Ln^{III} contain-

Abstract in Romanian: *Derivaţii carboxilici (+)- şi (−)-HL de tip pinen bipiridină sunt liganzi chirali capabili de a forma in reacţie cu ionii trivalenţi de lanthanide (Ln) structuri supramoleculare stabile. Intr-adevăr, procesul de auto-asamblare între aceşti liganzi enantiopuri L^- si ionii Ln^{III} (La, Pr, Nd, Sm, Eu, Gd, Tb, Dy, Ho, Er) are ca rezultat formarea unei arhitecturi trinucleare cu formula $[Ln_3(L)_6(\mu_3\text{-}OH)(H_2O)_3](ClO_4)_2$, abreviată ca tris(Ln[L]$_2$). Această nouă clasă de compuşi de simetrie C_3 a fost caracterizată atât în stare solidă cât şi în soluţie. Analizele de masă şi cele RMN au arătat că speciile trinucleare descrise în stare solidă sunt stabile in soluţie (solvent CH_2Cl_2) în limitele concentraţiilor testate (10^{-2} M–10^{-6} M). Proprietăţile fotofizice ale liganzilor enantiomeri HL şi ale complecsilor lor tris(Ln[L]$_2$) au fost studiate atât la temperatura camerei cât şi la 77 K demonstrând că anumiţi compuşi emit în infraroşu sau vizibil. Proprietatile chiroptice ale complecşilor tris(Ln[L]$_2$) au fost studiate prin spectroscopia de dicroism circular (DC) şi prin cea de luminescenţă circular polarizată (LCP). O activitate intensă este observată în regiunea tranziţiilor π-π* ale bipiridinei. Spectrele LCP ale tris(Eu[(+)-L]$_2$) şi tris(Tb[(+)-L]) prezintă valori importante ale factorilor de disimetrie g_{em} pentru tranziţiile senzitive ale Eu^{III} ($^5D_0 \rightarrow {}^7F_1$, $g_{em} = -0.088$) şi Tb^{III} ($^5D_4 \rightarrow {}^7F_5$, $g_{em} = -0.0806$). Proprietătile de auto-recunoaştere chirală ale sistemului descris aici au fost studiate folosind diferite amestecuri enantiomerice ale ligandului. Spectrele RMN (identice cu cele ale complecşilor enantiopuri) ca şi investigatiile prin spectroscopie DC arată că autorecunoaşterea chirală în procesul de auto-asamblaj este aproape totală. Aceasta are ca rezultat formarea exclusivă a structurilor homochirale de tip trinuclear.*

Abstract in Italian: *I derivati carbossilici della pinen-bipiridina (+)- e (−)-HL, sintetizzati per formare complessi configurazionalmente stabili con ioni lantanidi, hanno provato la loro efficacia come building blocks chirali nella sintesi di strutture supramolecolari contenenti lantanidi. Infatti un processo di auto assemblaggio completamente diastereoselettivo ha luogo tra il legante enantiomericamente puro L^- e ioni Ln^{III} (La, Pr, Nd, Sm, Eu, Gd, Tb, Dy, Ho, Er). Questo conduce alla formazione quantitativa di architetture supramolecolari trinucleari di formula generale $[Ln_3(L)_6(\mu_3\text{-}OH)(H_2O)_3](ClO_4)_2$ (abbreviato in tris(Ln[L]$_2$). La struttura di questa classe di composti a simmetria C_3 è stata caratterizzata in stato solido e in soluzione. Analisi ES-MS e ^{1}H-NMR indicano che le specie trinucleari sono stabili in soluzione (CH_2Cl_2), nell'intervallo di concentrazioni investigato (10^{-2} M–10^{-6} M). Le proprietà fotofisiche del legante HL e dei suoi complessi tris(Ln[L]$_2$) sono state studiate a temperatura ambiente e a 77 K, evidenziando una buona sensitizzazione da parte del legante sui centri metallici emettitori nel visibile e nel vicino infra-rosso (NIR).Le proprietà ottiche chirali dei complessi sono state investigate a mezzo di Dicroismo Circolare (CD) e Luminescenza Circolarmente Polarizzata (CPL). Una consistente attività CD è rilevata nella regione delle transizioni π–π* della bipiridina. Gli spettri CPL dei complessi tris(Eu[(+)-L]$_2$) e tris(Tb[(+)-L]$_2$) presentano fattori di dissimetria g_{em} elevati in corrispondenza delle transizioni sensibili degli ioni Eu^{III} ($^5D_0 \rightarrow {}^7F_1$, $g_{em} = -0.088$) e Tb^{III} ($^5D_4 \rightarrow {}^7F_5$, $g_{em} = -0.0806$). Le capacità di auto-riconoscimento del sistema sono state studiate in presenza di miscele artificiali degli enantiomeri del legante. Spettri ^{1}H-NMR identici a quelli dei complessi enantiomericamente puri e studi di spettroscopia CD hanno rivelato un auto-riconoscimento chirale pressoché completo nel processo di auto-assemblaggio che porta, di conseguenza, a miscele di complessi trinucleari omochirali.*

ing compounds with higher nuclearity—actually dinuclear helicates—have been reported.[22,23] As a result of the proven effectiveness shown by the pinene-type ligands in the predetermination of configuration in complexes with d transition metals,[24] we sought to extend their use to the lanthanide series. Considering the strong oxophilic character of the Ln^{III} ions, our approach is to adapt the binding site by incorporating a carboxylic unit into the pinene bipyridine framework.[25] The introduction of this new functionality to the pinene moiety is realized by a diastereoselective substitution reaction that has the advantage of creating a new, predetermined carbon stereocenter which will strengthen the chiral induction capability. The two enantiomers (+)-HL and (−)-HL of such a ligand derived from 5,6-pinene-bipyridine have been obtained by using this synthetic strategy. Herein, we report the full characterization of this ligand and its ability to diasteleoselectively form an enantiopure trinuclear helical architecture with the general formula $[Ln_3(L)_6(\mu_3\text{-}OH)(H_2O)_3](ClO_4)_2$, hereinafter called tris(Ln[L]$_2$), in the presence of Ln^{III} ions (La, Pr, Nd, Sm, Eu, Gd, Tb, Dy, Ho, Er) (Scheme 1). Two compounds belonging to this class have been included in two preliminary reports.[26,27] Detailed structural investigations along the lanthanide series in the solid state and solution and the photophysical and chiroptical properties are presented. Special emphasis is given to the investigation of the chiral-recognition properties of the self-assembly process when enantiomeric mixtures of (+)-HL or (−)-HL are used.

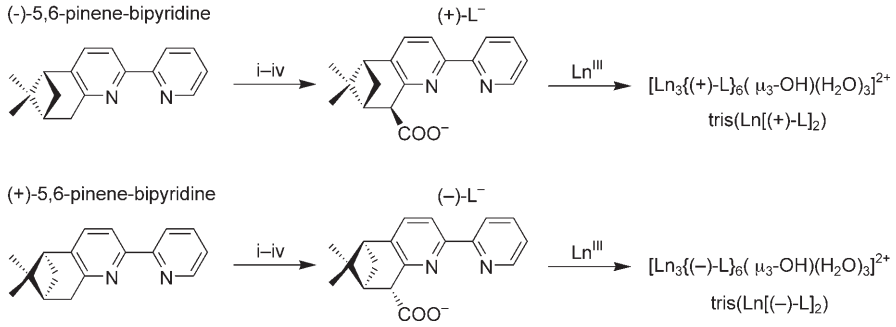

Scheme 1. Synthesis from 5,6-pinene bipyridine precursor of the ligand L^- enantiomers and their trinuclear, enantiopure complexes. i) diisopropylamine (LDA), −40 °C; ii) CO_2; iii) HCl; iv) TEA.

Results and Discussion

Synthesis and characterization of the enantiomeric ligands (+)- and (−)-HL: The ligand (+)-HL·HCl and its enantiomer (−)-HL·HCl were obtained by functionalization of the pinene framework of (−)- and (+)-5,6-pinene-bipyridine, respectively.[28] After the regio- and stereoselective deprotonation of the methylene group in the α position to the pyridine ring, the nucleophilic attack of CO_2 led to the formation of the target molecule.[26] The ligand was isolated in acidic medium to prevent the decarboxylation process typical for β-immino acids in the neutral form.[29] The X-ray structure of the adduct with hydrochloric acid (+)-HL·HCl reveals the characteristic *cis* conformation adopted by monoprotonated bipyridines (Figure 1).[30] The two pyridine rings are almost coplanar (dihedral angle = 3.24°). The hydrogen-bonding interactions between the two nitrogen atoms and water molecule of crystallization are mainly responsible for the coplanarity, which is enforced by the offset π–π and CH···π stacking between neighboring molecules in the crystal (Figure 2). The bond lengths and angles determined in this structure are consistent with those reported for similar 5,6-pinene-bipyridine derivatives.[31]

The ^{1}H NMR spectrum of (+)-HL·HCl is assigned on the basis of coupling constants and ^{1}H–^{1}H COSY correlations. The ^{1}H NMR spectrum of the anion form (+)-L^- was also measured after deprotonation in situ with two equivalents of triethylamine (TEA) as the base. The differences in chemical shifts (more pronounced in the aromatic region) account for the magnetic changes induced by the *cis*→*trans* isomerization of the bipyridine moiety (see the Experimental Section).[32]

Preparation and solid-state characterization of tris(Ln[L]$_2$) Reaction in methanol of (+)-, (−)-, and racemic (±)-HL with $Ln(ClO_4)_3{\cdot}x\,H_2O$ salts (Ln^{III} = La, Pr, Nd, Sm, Eu, Gd, Tb, Dy, Ho, Er; metal/ligand = 1:2) in the presence of TEA leads to the straightforward and virtually quantitative formation of a precipitate. Elemental analyses of the amorphous precipitates are in agreement with the general formula $[Ln_3L_6(\mu_3\text{-}OH)(H_2O)_3](ClO_4)_2{\cdot}x\,H_2O$ (see the Experimental Section). These compounds are soluble in chlorinated solvents, acetonitrile, ni-

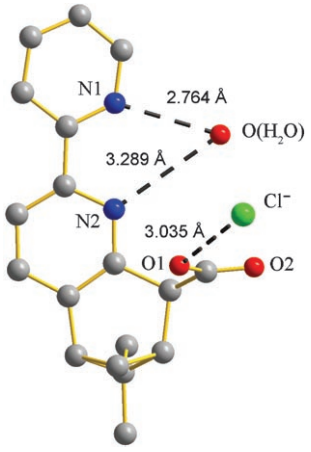

Figure 1. X-ray structure of (+)-HL·HCl·H_2O. Dotted lines: O···N, O···Cl relative distances.

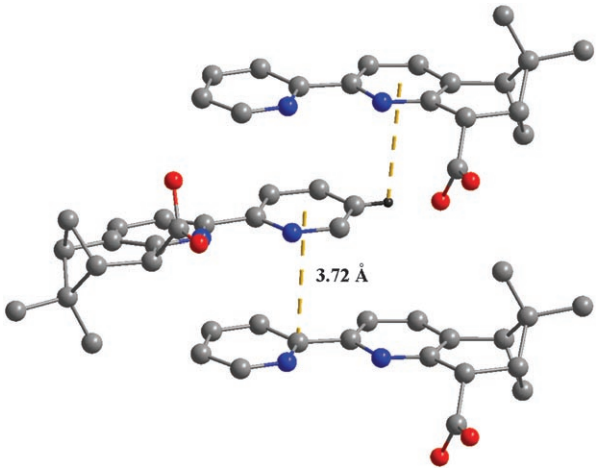

Figure 2. Crystal packing of (+)-HL·HCl·H_2O showing the offset π–π stacking between two consecutive bipyridine moieties.

tromethane, and acetone but poorly soluble in alcoholic or aqueous media. The reaction of the latter three Ln^{III} ions in the series (Tm, Yb, and Lu) led instead to the formation of an insoluble precipitate that is likely polymeric in nature.

X-ray analyses of crystals grown by slow evaporation of the hydrated acetonitrile solutions gave isostructural complexes of the general formula $[Ln_3L_6(\mu_3\text{-}OH)(H_2O)_3](ClO_4)_2 \cdot x\,H_2O \cdot y\,CH_3CN$ (La^{III}: $x=1$, $y=0$; Pr^{III}: $x=3$, $y=4$; Nd^{III}: $x=5$, $y=10$; Sm^{III}: $x=3$, $y=7$; Eu^{III}: $x=3$, $y=0$; Gd^{III}: $x=3$, $y=4$; Tb^{III}: $x=3$, $y=8$; Dy^{III}: $x=5$, $y=10$; Ho^{III}: $x=3$, $y=0$; Er^{III}: $x=3$, $y=0$). The crystallographic data are given in Table 1.

All the structures possess a crystallographic C_3 axis and consist of a trimetallic core and six ligands wrapped around, three by three, in a helical opposite fashion. The Ln^{III} ions define the corners of an equilateral triangle, with a side of about 4 Å, progressively decreasing with the ionic radius of the Ln^{III} centers (Table 2). The three metal centers are equidistantly bound to a μ_3-bridging hydroxide ion that lies on the C_3 axis and is displaced by about 0.9 Å from the plane defined by the three Ln^{III} ions. The six ligands around the metal core are grouped into two sets. The first set of three ligands (set **S** - green in Figures 3 and 4) coordinates through two bipyridine nitrogen atoms and the carboxylate group that binds two metal centers in a μ^3–η^2:η^1 fashion. They display an *M* propeller-like arrangement. The ligands of the second set (**S′**: orange in Figures 3 and 4) wrap around the trimetallic core in a *P*-helical fashion and coordinate solely through the carboxylate groups, which bridge two metal centers in a symmetric μ^2–η^1:η^1 mode. The *P*- and *M*-helical arrangements described above are adopted if the (+)-L^- enantiomer is used (Figure 5a). On the other hand, when employing the (−)-L^- enantiomer, the opposite configuration is obtained (the *P* helix is formed by the ligands of set **S** and the *M* helix from set **S′**; Figure 5b).

The bipyridine groups of the ligands that belong to set **S**, which coordinate through both the nitrogen atoms, consequently present a *cis* conformation. The dihedral angle between the averaged planes of the pyridine rings is smaller than 20° for all of the complexes and close to coplanarity in the case of tris(Eu[(+)-$L]_2$) (see Table 3). Considering that the ligands belong to set **S′**, the *cis* conformation is maintained although the bipyridine moiety is not involved in coordination and the *trans* conformation should be energetically favored.[33] The *cis* conformation is nevertheless preferred as result of a hydrogen-bonding network that connects the nitrogen atoms of the bipyridine moiety, the water molecule of crystallization, and the water molecule coordinated to the metal ion (Figure 6a). In the case of the La^{III} ion, no water of crystallization is detected in the cavity formed by the ligands of set **S′** and therefore the ligands adopt a *transoid* conformation (Figure 6b). In this case, the dihedral angle between the planes that contain the pyridine rings is 154°, in accordance with the value of 152° calculated from the dipole moment of free bipyridine.[34]

The coordination sphere around each nine-coordinated Ln^{III} ion is composed of two bipyridine nitrogen atoms, five carboxylic oxygen atoms, one oxygen atom from water, and one oxygen atom from the μ_3-OH group (Figure 6). The bond lengths from the lanthanide ions to the coordinating nitrogen and oxygen atoms are reported in Table 2. With two exceptions (Eu and Dy), a slight shortening of bond length (<10%) is observed along the lanthanide series as a result of the higher charge density on smaller ions.

In all the cases, the bond length involving the nitrogen atom of the pinene-condensed pyridine cycle (Ln−N16) is longer than the one concerning the nitrogen atom from the pinene-free pyridine cycle (Ln−N1). These relatively long bond lengths Ln−N16 (2.85–2.75 Å) are, however, comparable with those reported for other Ln^{III}–bipyridine coordination compounds.[35–38] The geometry of the coordination polyhedra is intermediate between the tricapped trigonal prism and the capped square antiprism, which are the common geometries for the coordination number nine. A complete, quantitative comparison between the structures reported herein and these idealized geometries would require a computational shape analysis, as exemplified by Raymond and co-workers.[39]

The IR spectra recorded of the crystalline powder and the amorphous precipitates were found to be the same, thus confirming their identical nature. The spectra of all of the complexes (see the Supporting Information) are characterized by a large band centered at 3290 cm^{-1}, which accounts for the presence of water in the structure. The shoulder at 3560 cm^{-1} corresponds instead to the stretching frequency ν(O−H) of the μ_3-OH group. A strong band present at 1094 cm^{-1} can be ascribed to the presence of uncoordinated perchlorates.[40] The strong band at 1610 cm^{-1} is characteristic of the asymmetric stretching frequency $\nu(COO)_{as}$ of the O-C-O bonds within the carboxylic moieties, whereas the two bands at 1420 and 1385 cm^{-1} correspond to the symmetrical stretching frequency $\nu(COO)_s$. According to theory,[41,42] the difference in shift $\Delta(\nu_{as}-\nu_s)$ can be correlated with the coordination mode of the carboxylic group. We calculated two different $\Delta(\nu_{as}-\nu_s)$ values: the first of about

Table 1. Crystallographic data for ligand (+)-HL·HCl and the trinuclear complexes of the general formula $[Ln_3L_6(\mu_3\text{-}OH)(H_2O)_3](ClO_4)_2\cdot x\,H_2O\cdot y\,CH_3CN$.

	(+)-HL-HCl	tris(La[(−)-L]$_2$)	tris(Pr[(+)-L]$_2$)	tris(Nd[(−)-L]$_2$)	tris(Sm[(+)-L]$_2$)	tris(Eu[(+)-L]$_2$)
formula	$C_{18}H_{21.5}ClN_2O_3$	$C_{108}H_{111}Cl_2La_3N_{12}O_{25}$	$C_{116}H_{127}Cl_2Pr_3N_{16}O_{27}$	$C_{128}H_{147}Cl_2Nd_3N_{22}O_{31}$	$C_{122}H_{136}Cl_2Sm_3N_{19}O_{27}$	$C_{108}H_{115}Cl_2Eu_3N_{12}O_{27}$
fw [g mol^{-1}]	353.32	2464.72	2670.97	2993.30	2822.45	2539.90
T [K]	140(2)	173(2)	100(2)	173(2)	173(2)	140(2)
crystal system	triclinic	trigonal	hexagonal	hexagonal	hexagonal	rhombohedral
space group	$P1$	$R3$ (No.146)	$P6_3$ (No.173)	$P6_3$ (No.173)	$P6_3$ (No.173)	$R3$
θ range [°]	2.95–25.03	3.3–22.0	2.7–26.0	1.3–27.5	1.3–25.3	2.8–25.0
crystal description	prismatic	cube	prismatic	hexagonal	Block	prismatic
color	colorless	colorless	pale green	colorless	colorless	colorless
crystal size [mm^3]	0.14×0.09×0.07	0.10×0.10×0.10	0.24×0.18×0.12	0.54×0.41×0.36	0.35×0.40×0.50	0.31×0.17×0.17
F(000)	373	3744	2724	3062	2874	3858
a [Å]	7.3667(9)	19.6189(14)	17.7054(4)	17.829(2)	17.7025(12)	17.3468(11)
b [Å]	8.701(2)	19.6189(14)	17.7054(4)	17.829(2)	17.7025(12)	17.3468(11)
c [Å]	14.267(3)	26.770(2)	24.0794(7)	24.0536(14)	23.9875(19)	30.846(4)
α [°]	104.45(2)	90.00	90.00	90.00	90.00	90.00
β [°]	92.607(13)	90.00	90.00	90.00	90.00	90.00
γ [°]	91.010(16)	120.00	120.00	120.00	120.00	120.00
V [Å^3]	884.2(3)	8923.4(11)	6537.1(3)	6621.6(11)	6510.1(8)	8038.3(13)
Z	2	3	2	2	2	3
reflections measured	5317	14391	41149	51222	44045	16262
unique reflections	4632	4733	7739	9984	7816	6240
$R^{[a]}$, $wR^{[b]}$ [$I>2\sigma(I)$]	0.0605, 0.1530	0.0645, 0.1253	0.0470, 0.1341	0.0380, 0.1028	0.0427/0.1050	0.0535, 0.0915
$R^{[a]}$, $wR^{[b]}$ (all data)	0.0908, 0.1421	0.1069, 0.1377	0.0724, 0.1570	0.0531, 0.1110	0.0493/0.1087	0.1049, 0.1189
goodness-of-fit$^{[c]}$ (F^2)	0.898	0.815	0.973	1.049	1.034	0.811
diffraction limits	$-7<h<7$	$-20<h<20$	$-21<h<21$	$-23<h<20$	$-21<h<21$	$-20<h<20$
	$-10<k<10$	$-20<k<20$	$-19<k<21$	$-20<k<22$	$-21<k<21$	$-20<k<20$
	$-16<l<16$	$-26<l<28$	$-22<l<29$	$-31<l<30$	$-28<l<28$	$-34<l<36$
data/param/restraints	4632/442/3	4733/453/14	7739/497/18	9984/461/1	7816/461/1	6240/445/162
ρ_{calcd} [g cm^{-3}]	1.327	1.376	1.357	1.501	1.287	1.574
μ [mm^{-1}]	0.236	1.174	1.213	1.282	1.453	1.865
completeness to θ_{max} [%]	87.5	99.6	99.8	99.7	98.8	99.9
largest diff. peak hole [Å^{-3}]	0.481, −0.281	1.50, −0.74	2.41, −0.87	1.73, −0.97	−0.69, 0.71	1.243, −0.723

	tris(Gd[(+)-L]$_2$)	tris(Tb[(+)-L]$_2$)	tris(Dy[(−)-L]$_2$)	tris(Ho[(−)-L]$_2$)	tris(Er[(−)-L]$_2$)	tris(Eu[(±)-L]$_2$)[a]
formula	$C_{108}H_{115}Cl_2Gd_3N_{12}O_{27}$	$C_{124}H_{139}Cl_2Tb_3N_{20}O_{27}$	$C_{128}H_{153}Cl_2Dy_3N_{22}O_{31}$	$C_{108}H_{115}Cl_2Ho_3N_{12}O_{16}$	$C_{108}H_{115}Cl_2Er_3N_{12}O_{16}$	$C_{125.5}H_{139.75}ClEu_3F_3N_{20.25}O_{22}S$
fw [g mol^{-1}]	2719.99	2889.21	3054.12	2578.81	2585.80	2864.22
T [K]	173(2)	173(2)	173(2)	173(2)	173(2)	140(2)
crystal system	hexagonal	hexagonal	hexagonal	trigonal	trigonal	triclinic
space group	$P6_3$ (No.173)	$P6_3$ (No.173)	$P6_3$ (No.173)	$R3$ (No 146)	$R3$	$P\bar{1}$ (No. 2)
θ range [°]	1.6–25.7	1.6–25.7	1.3–27.5	1.50–25.15	1.48–25.12	2.8–26.0
crystal description	block	plate	block	block	block	prismatic
color	colorless	colorless	colorless	pale pink	pale pink	colorless
crystal size [mm^3]	0.26×0.30×0.45	0.26×0.45×0.45	0.30×0.38×0.43	0.40×0.25×0.20	0.30×0.25×0.15	0.17×0.22×0.23
F(000)	2754	2736	2622	3894	3903	2919
a [Å]	17.756(3)	17.7054(4)	17.7560(16)	17.9789(8)	17.9969(6)	16.6740(10)
b [Å]	17.756(3)	17.7054(4)	17.7560(16)	17.9789(8)	17.9969(6)	22.3910(10)
c [Å]	24.099(5)	24.0794(7)	24.099(2)	29.4923(14)	29.5199(14)	22.524(2)
α [°]	90.00	90.00	90.00	90.00	90.00	62.148(6)
β [°]	90.00	90.00	90.00	90.00	90.00	72.637(6)
γ [°]	120.00	120.00	120.00	120.00	120.00	80.615(5)
V [Å^3]	6580(2)	6537.1(3)	6579.9(10)	8255.9(7)	8280.2(6)	7093.6(9)
Z	2	2	2	3	3	2
reflections measured	27646	91960	45867	27183	27122	46368
unique reflections	8280	11807	9942	6329	6553	24114
$R^{[a]}$, $wR^{[b]}$ [$I>2\sigma(I)$]	0.0349, 0.0891	0.0312, 0.0668	0.0350, 0.0934	0.0501, 0.1359	0.0489, 0.1306	0.0760, 0.2036
$R^{[a]}$, $wR^{[b]}$ (all data)	0.0436, 0.0921	0.0424, 0.0698	0.0493, 0.0996	0.0524, 0.1383	0.0711, 0.1417	0.1141, 0.2249
goodness-of-fit$^{[c]}$ (F^2)	1.015	0.975	1.055	1.037	1.017	1.002
diffraction limits	$-21<h<13$	$-24<h<24$	$-18<h<22$	$-21<h<21$	$-21<h<21$	$-20<h<20$
	$-20<k<21$	$-23<k<24$	$-22<k<16$	$-21<k<21$	$-19<k<21$	$-24<k<25$
	$-29<l<29$	$-32<l<33$	$-31<l<31$	$-35<l<31$	$-35<l<35$	$-27<l<27$
data/param/restraints	8280/508/19	11807/457/1	9942/470/3	6329/337/1	6553/337/1	24114/1580/56
ρ_{calcd} [g cm^{-3}]	1.373	1.378	1.316	1.549	1.548	1.341
μ [mm^{-1}]	1.607	1.724	1.810	2.263	2.387	1.416
completeness to θ_{max} [%]	99.0	98.7	99.7	99.5	99.5	86.4
largest diff. peak hole [Å^{-3}]	1.66, −0.62	2.12, −1.36	1.29, −0.71	−1.14, 1.23	−1.16, 1.28	−3.94, 4.22

[a] Racemate of general formula $[Eu_3\{(\pm)\text{-}L\}_6(\mu_3\text{-}OH)(H_2O)_3](CF_3SO_3)(Cl)\cdot 3\,H_2O\cdot 8\,CH_3CN$.

Table 2. Selected distances [Å] within the first coordination sphere of Ln^{III} ions.[a]

	Ln	COO^- (set **S**)		Bipyridine (set **S**)		COO^- (set **S′**)				Ln···Ln distance	OH–Ln plane
		O21	O21	O22	N1	N16	O44	O43	O_{OH}	O_{H_2O}		
enantiopure tris(Ln[L]$_2$) complexes	La	2.35(2)	2.54(2)	2.68(2)	2.64 (2)	2.85(2)	2.464(2)	2.42(2)	2.56(1)	2.55(2)	4.127(1)	0.94(3)
	Pr	2.356(6)	2.516(5)	2.701(6)	2.620(7)	2.827(7)	2.421(4)	2.395(5)	2.515(3)	2.550(8)	4.0396(6)	0.943(8)
	Nd	2.357(3)	2.516(4)	2.673(4)	2.612(4)	2.831(6)	2.394(4)	2.412(4)	2.510(2)	2.523(4)	4.0337(4)	0.936(5)
	Sm	2.320(4)	2.455(3)	2.647(5)	2.577(5)	2.768(5)	2.358(4)	2.369(7)	2.471(2)	2.485(5)	3.9679(3)	0.927(5)
	Eu	2.298(9)	2.45(2)	2.668(9)	2.51(2)	2.767(2)	2.379(8)	2.332(9)	2.412(6)	2.502(7)	3.915(2)	0.84(2)
	Gd	2.294(4)	2.443(4)	2.609(4)	2.542(7)	2.775(5)	2.344(3)	2.347(3)	2.440(2)	2.446(4)	3.9285(8)	0.904(5)
	Tb	2.279(3)	2.437(3)	2.614(3)	2.534(3)	2.758(3)	2.323(3)	2.323(4)	2.434(2)	2.449(3)	3.9077(3)	0.915(4)
	Dy	2.292(4)	2.439(3)	2.608(4)	2.555(3)	2.771(5)	2.326(4)	2.328(5)	2.439(2)	2.456(4)	3.9190(3)	0.910(5)
	Ho	2.269(7)	2.403(8)	2.590(9)	2.47(1)	2.71(1)	2.304(9)	2.356(9)	2.389(4)	2.441(6)	3.8565(5)	0.866(9)
	Er	2.254(7)	2.396(8)	2.570(9)	2.473(2)	2.70(2)	2.292(9)	2.347(9)	2.436(6)	2.382(4)	3.8413(4)	0.870(9)
racemate tris(Eu[(±)-L]$_2$)	Eu1	2.300(7)	2.447(7)	2.565(9)	2.547(8)	2.789(7)	2.461(6)	2.409(8)	2.367(9)	2.448(7)	3.9427(7)[b]	
	Eu2	2.313(8)	2.548(7)	2.477(7)	2.512(2)	2.826(8)	2.460(8)	2.397(6)	2.343(5)	2.465(9)	3.9513(8)[c]	0.918(7)
	Eu3	2.381(8)	2.451(7)	2.520(8)	2.537(9)	2.77(1)	2.481(8)	2.406(8)	2.299(5)	2.455(8)	3.9484(6)[d]	

[a] For the numbering scheme, see Figure 4. [b] Eu1···Eu2 distance. [c] Eu2···Eu3 distance. [d] Eu1···Eu3 distance.

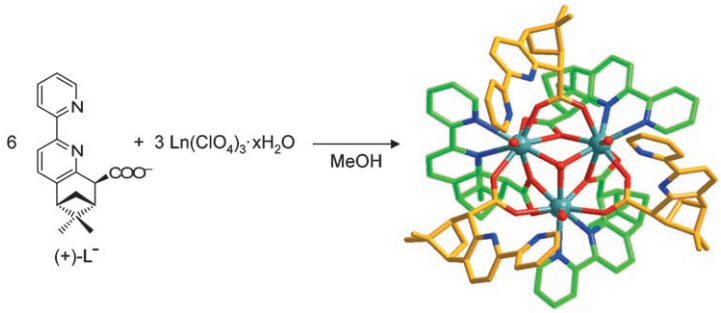

Figure 3. Self-assembly leading to the trinuclear Ln^{III} array, tris(Ln[L]$_2$). Structure of the molecular cation $[Sm_3\{(+)\text{-}L\}_6(\mu_3\text{-}OH)(H_2O)_3]^{2+}$ is viewed parallel to the C_3 axis. Ligands belonging to set **S** are shown in green; those belonging to set **S′** are shown in orange (see text); O: red, N: blue, Sm: blue–green.

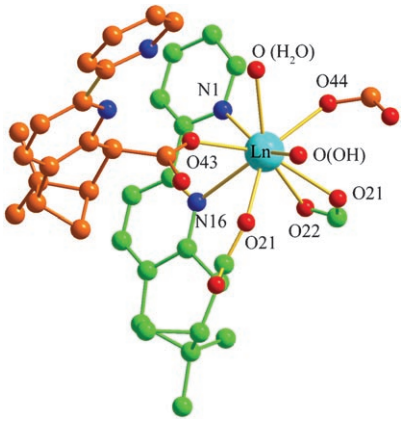

Figure 4. Numbering scheme of the atoms in the first coordination sphere of the Ln^{III} ions in the C_3-symmetrical tris(Ln[L]$_2$) complexes.

225 cm^{-1} can be ascribed to a bidentate-bridging binding mode, which is the case of carboxylic groups in set **S′**; the second of about 190 cm^{-1} may indicate a coordination mode intermediate between the bidentate-cyclic and bidentate-bridging modes, which are both characteristic for set **S** as observed by X-ray studies.

Characterization in solution: The ES mass spectra display only two peaks unambiguously assigned to the molecular cations $[Ln_3L_6(OH)]^{2+}$ and their monocharged perchlorate adducts $[Ln_3L_6(OH)(ClO_4)]^+$. A weaker signal that corresponds to $[Ln_3L_6(OH)(H_2O)]^{2+}$ was detected in a few cases as a consequence of the fragmentation during the ionization process. The spectra of the La^{III}, Eu^{III}, and Er^{III} complexes are representative for all of the complexes along the lanthanide series (Figure 7).

Characterization by NMR spectroscopic analysis is limited to the complexes formed with Ln^{III} ions, which as a result of their absent (La^{III}) or low paramagnetism (Pr^{III}, Nd^{III}, Sm^{III} and Eu^{III}) allowed a good resolution of the spectra. A total of 26 resonances spread over different spectral domains according to the specific Ln^{III} ion employed are observed in the ^1H NMR spectra (Figure 8). Large paramagnetic shifts (up to $\Delta\delta = 18$ ppm in the case of the Pr^{III} and Nd^{III} complexes) characterize the signals of those protons located close to the binding site. This behavior is the case, for example, of the H1, H13, and H13′ signals (for the numbering scheme see Figure 8), which are also affected by significant line broadening and subsequent loss of couplings with other nearby protons. The line assignment (Table 4), achieved by 2D techniques (COSY, TOCSY, and ROESY), allowed us to group the signals into two sets of 1:1 ratios, each set accounting for 13 resonances. Considering that the ligand displays also 13 signals, the two sets determined before clearly correspond to the two magnetically nonequivalent ligand types (sets **S** and **S′**) observed by X-ray studies (see above). Moreover, important structural information was provided by intra- and interligand NOE interactions observed in

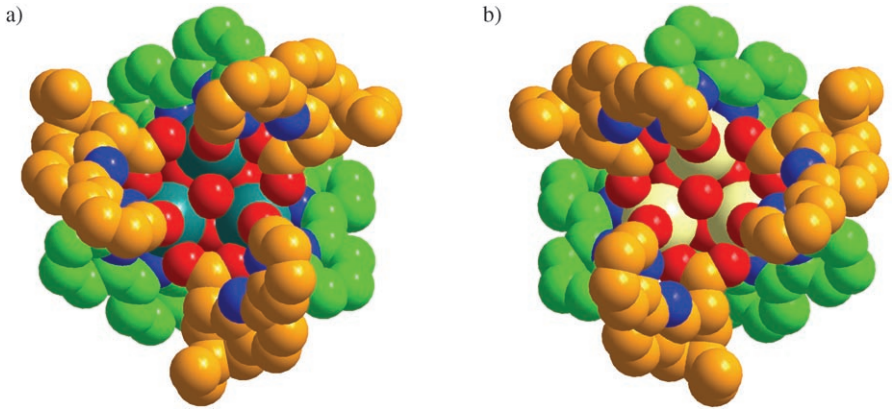

Figure 5. Space-filling representation of a) tris(Tb[(+)-L]$_2$) and b) tris(Dy[(−)-L]$_2$) viewed parallel to the C_3 axis and showing the opposite helical arrangement of the enantiomeric ligands. Tb: dark green, Dy: light yellow, N: blue, O: red, ligand set **S**: light green, ligand set **S′**: orange.

Table 3. Dihedral angles of the bipyridine moieties in the complexes and in the free ligand.

		Dihedral angle θ [°]		Distance N1−OH$_2$ [Å][a]
	Ln	Set **S**	Set **S′**	
Enantiopure tris(Ln[L]$_2$) complexes	La	16.4(6)	153.8(7)	–
	Pr	19.9(3)	36.7(3)	3.20(2)
	Nd	19.8(2)	37.0(3)	3.228(6)
	Sm	19.2(3)	35.7(3)	3.18(1)
	Eu	4.0(5)	11.3(4)	2.86(2)
	Gd	18.8(2)	38.1(3)	3.21(1)
	Tb	19.2(2)	19.1(1)	3.206(6)
	Dy	20.3(2)	36.5(2)	2.984(6)
	Ho	9.3(5)	29.7(7)	3.4(2)
	Er	9.6(5)	29.3(9)	3.4(2)
Racemate tris(Eu[(±)-L]$_2$)	Eu1	19.3(4)	162.4(5)	
	Eu2	21.8(4)	144.0(4)	
	Eu3	19.5(4)	158.3(6)	–
(+)-HL·HCl		3.2(3)		2.764(9)

[a] Water molecule of crystallization.

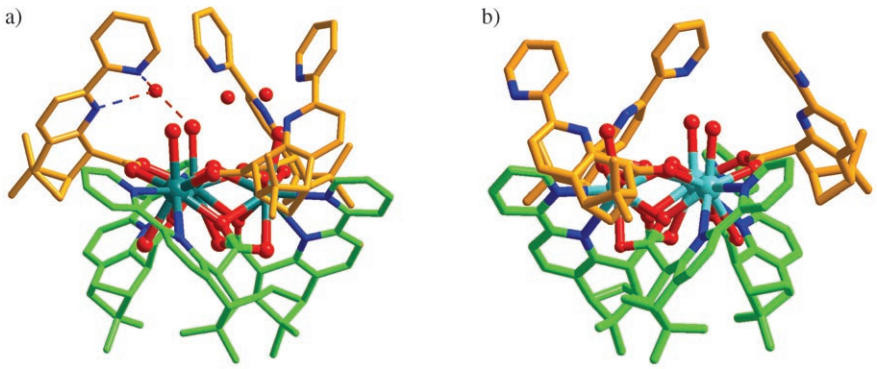

Figure 6. X-ray structures of a) tris(Pr[(+)-L]$_2$) and b) tris(La[(−)-L]$_2$) viewed perpendicularly to the C_3 axis. Note the *trans* conformation of the uncoordinated bipyridine moieties in the structure of the La^{III} complex. In the structure of the Pr^{III} complex, the water molecules of crystallization and the hydrogen-bonding network that stabilizes the *cis* conformation are represented. La: turquoise, Pr: blue–green, N: blue, O: red, ligand set **S**: light green, ligand set **S′**: orange.

ROESY spectra, which helped to assign the two sets. In fact, the intraligand cross peak between the two aromatic protons H4/H7 that belong to the two pyridine rings is detected only in the case of set **S**, as a consequence of the *cis* conformation adopted by the coordinated bipyridine moieties. This magnetic interaction is missing in set **S′**, in which the uncoordinated bipyridines adopt a *trans* conformation in solution. In addition, relevant interligand NOE interactions confirmed the H···H distances measured in the solid state, thus giving strong proof of the maintenance of the trinuclear structures in solution (Table 5). In the case of the most paramagnetic complexes, some of these cross peaks are lost as result of the proximity of the corresponding nuclei to the paramagnetic centers or simply because of the overlap of the signals. It is worth mentioning that besides the assigned resonances, only traces of minor signals (<5%) are detected, thus accounting for the high diastereoselectivity of the self-assembly process.

Photophysical properties: The absorption spectrum of the anionic form of (+)-L$^-$ in CH_2Cl_2 shows two absorption bands centered at 34130 (293 nm, π_1) and 40000 cm^{-1} (250 nm, π_2), ascribed to $\pi\rightarrow\pi^*$ transitions mainly located on the pyridine units, although also contributions from the carboxylic moiety should be invoked for the most energetic transition.[43]

In the spectra of the tris(Ln[L]$_2$) complexes the main band π_1 appears red-shifted to around 33000 cm^{-1} (303 nm, red-shift ≈1127 cm^{-1}), thus accounting for a *trans*→*cis* isomerization of L$^-$ upon complexation (see the Supporting Information).[30,32] The ε values are consistent along the lanthanide series and are roughly six times higher than the ε value of the corresponding maxima of the free ligand, which supports the presence of six bipyridine units per molecule of complex.

Ligand-centered emission: Upon excitation at 36363 cm^{-1} (275 nm) of a solution of (+)-H_2L^+ in CH_2Cl_2, the $^1\pi\pi^*$ singlet-state emission band appears centered around 25800 cm^{-1} (387 nm; Figure 9). At low temperature (77 K), the emission of the singlet is ac-

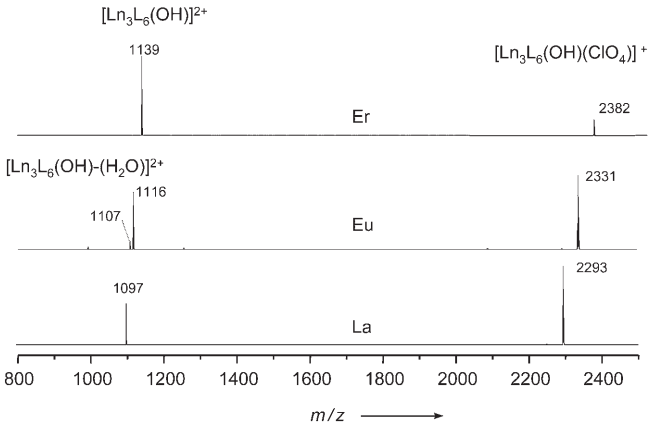

Figure 7. Examples of the ES-MS spectra of some tris(Ln[L]$_2$) complexes (CH_2Cl_2, $c \approx 3\times10^{-4}$ M).

companied by the emission of the triplet state $^3\pi\pi^*$ centered at 20490 cm^{-1} (488 nm). The triplet band appears structured in a vibrational progression of (1410 ± 50) cm^{-1} with the 0–phonon transition at 21930 cm^{-1} (456 nm). The ligand-centered luminescence in the Gd^{III} complex displays basically the same features observed in the free ligand with the singlet band slightly blue-shifted (maximum around 28500 cm^{-1}, 351 nm), thus confirming the suitability of this ligand as a sensitizer for Eu^{III} and Tb^{III} luminescence. The acceptor levels of these two ions ($^5D_0$ at 17300 cm^{-1} for Eu^{III} and $^5D_4$ at 20500 cm^{-1} for Tb^{III}) lie at lower energies with respect to the ligand $^3\pi\pi^*$ state, with $\Delta E(^3\pi\pi^* - ^5D_J)$ of 4630 and 1430 cm^{-1} for Eu^{III} and Tb^{III}, respectively.

Emission properties of visible (tris(Eu[(+)-L]$_2$) and tris(Tb[(+)-L]$_2$)) and near-infrared (NIR) (tris(Er[(−)-L]$_2$)

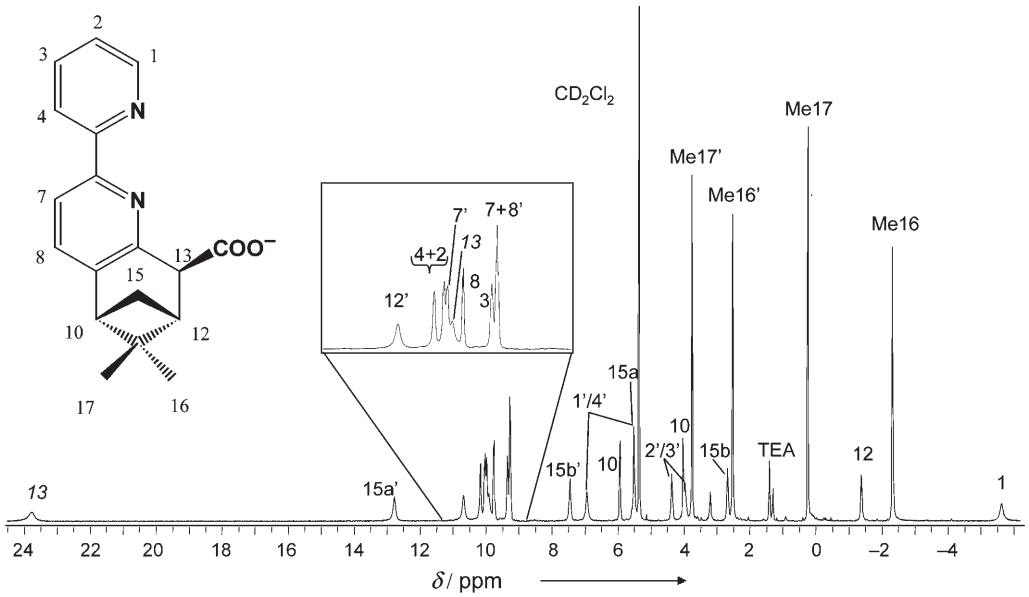

Figure 8. Numbering scheme for the ligand and ^{1}H NMR spectrum (CD_2Cl_2, RT, $c = 8\times10^{-3}$ M) of tris(Nd[(−)-L]$_2$) with attribution of the signals.

Table 4. Complete line assignment of the ^{1}H NMR spectra of tris(Ln[L]$_2$) complexes.[a]

	La		Pr		Nd		Sm		Eu	
	S	**S′**	**S**	**S′**	**S**	**S′**	**S**	**S′**	**S**	**S′**
H1	7.70	8.67	−11.10	3.43	−5.63	6.93[b]	10.48	8.33	13.33	11.69
H2	6.89	7.30	7.16	4.20	10.01	4.36[c]	7.29	6.95	3.23	9.23
H3	7.89	7.98	6.98	3.05	9.33	3.96[c]	8.12	7.29	6.47	10.99
H4	7.98	8.40	7.41	3.04	10.15	5.50[b]	8.27	7.45	4.57	11.64
H7	7.96	8.26	11.36	9.28	9.27	9.96	8.40	8.47	5.08	7.33
H8	7.63	7.56	12.43	11.26	9.75	9.27	7.90	7.90	5.58	5.49
H10	2.95	2.75	6.14	9.59	4.02	5.93	3.27	3.03	1.52	−0.39
H12	2.53	1.06	−4.61	26.24	−1.38	10.66	2.92	1.73	5.97	−11.72
H13	4.07	3.56	21.03	19.20	23.76	9.90	4.51	2.69	−7.38	−5.40
H15a	1.44	1.44	12.20	27.52	5.50	12.77	3.15	1.92	−2.27	−9.38
H15b	2.70	2.03	4.01	15.42	2.67	7.45	2.92	2.57	3.05	−3.44
Me16	0.53	0.48	−3.97	6.05	−2.32	2.52	0.87	0.00	3.51	−2.20
Me17	1.41	1.27	−0.35	7.62	0.23	3.75	1.74	1.16	2.55	−1.73

[a] CD_2Cl_2, $c \approx 8\times10^{-3}$ M; δ values are given in ppm; see Figure 8, for the numbering scheme. [b] It is possible to swap the H1/4 values. [c] It is possible to swap the H2/3 values.

Table 5. Detected ROESY interligand cross peaks (●) and respective H···H distances.[a]

ROESY cross peak	La	H···H distance [Å]	Pr	H···H distance [Å]	Nd	H···H distance [Å]	Sm	H···H distance [Å]	Eu	H···H distance [Å]
H2⇄H7′	●	2.9	●	3.0	●	3.2	●	3.2	●	3.8
H2⇄H8′	●	3.9	●	3.2	–	3.0	●	3.0	●	4.6
H8⇄Me17′	●	3.1	–	3.7	–	3.6	●	3.6	–	3.4
H1⇄H15a′	●	4.1	–	2.7	–	2.7	–	2.8	–	3.3

[a] Calculated from the X-ray structures of the tris(Ln[L]$_2$) complexes.

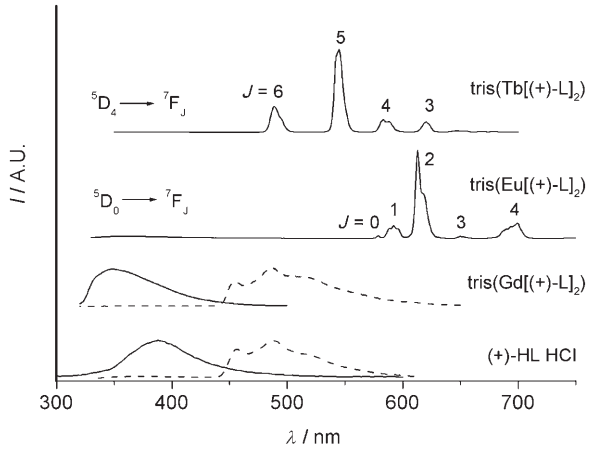

Figure 9. Emission spectra of ligand (+)-HL·HCl and its tris(Ln[(+)-L]$_2$) complexes in CH_2Cl_2 measured at room temperature (solid line, [L] = 5×10^{-5} M, [LnL] ≈ 1×10^{-6} M) and 77 K (dotted line, time-delay = 0.05 ms).

and tris(Nd[(−)-L$_2$]) emitters: An intense metal-centered luminescence is registered upon excitation at 275 nm of solutions of tris(Eu[(+)-L]$_2$) and tris(Tb[(+)-L]$_2$) in CH_2Cl_2. The characteristic $^5D_0 \rightarrow {}^7F_J$ (J = 0–4) transitions of Eu^{III} and the $^5D_4 \rightarrow {}^7F_J$ (J = 6–3) transitions of the Tb^{III} center dominate the respective spectra. Only an extremely weak residual emission from the $^1\pi\pi^*$ state of the ligand is observed in both cases (Figure 9). The emissions of the Eu^{III} and Tb^{III} compounds are characterized by a monoexponential decay and comparable quantum yields (Table 6). Among the synthesized tris(Ln[L]$_2$) complexes that are expected to display NIR emission (Ln^{III} = Pr, Nd, Sm, Ho, Dy, Er), only tris(Nd[(−)-L]$_2$) and tris(Er[(−)-L]$_2$) displayed a sizeable IR emission in solutions of CH_2Cl_2 (Figure 10). The tris(Er[(−)-L]$_2$) complex exhibits, as expected, a lower quantum yield (Table 6). This behavior is explained by a quenching of the luminescence through vibrational deactivations that are more effective in the case of the Er^{III} ion than in the case of the Nd^{III} ion, in virtue of the smaller energy gap between the luminescent and ground states. In the case of the Er^{III} center, the energy of the transition $^4I_{13/2} \rightarrow {}^4I_{15/2}$ is in the range 5500–6500 cm^{-1} and thus is easily quenched by the vibrations of C–H oscillators ($E \approx$ 2000–2500 cm^{-1}).[44–47] Luminescence decays are monoexponential and the values of the calculated lifetimes (see Table 6) are comparable with those reported for mononuclear Nd^{III} and Er^{III} complexes containing phenanthroline polyamino carboxylic-[48] and hydroxoquinolinate-type ligands.[44]

Table 6. Metal-centered emission properties of tris(Ln[L]$_2$) complexes (Ln^{III} = Eu, Gd, Tb, Er, Nd) in CH_2Cl_2.

Compounds	τ [ms]	Φ_{em} [%]
tris(Gd[(+)-L]$_2$)	4.1[a]	–
tris(Eu[(+)-L]$_2$)	1.6[b]	13
tris(Tb[(+)-L]$_2$)	0.71[c]	15
tris(Nd[(−)-L]$_2$)	0.60[d]	0.09
tris(Er[(−)-L]$_2$)	1.1[e]	0.013

[a] Relative to the triplet state (measured at 77 K). [b] The $^5D_0 \rightarrow {}^7F_2$ transition (615 nm; measured at RT). [c] The $^5D_4 \rightarrow {}^7F_5$ transition (540 nm; measured at RT). [d] The $^4F_{3/2} \rightarrow {}^4F_{11/2}$ transition (1063 nm; measured at RT). [e] The $^4I_{13/2} \rightarrow {}^4I_{15/2}$ transition (1525 nm; measured at RT).

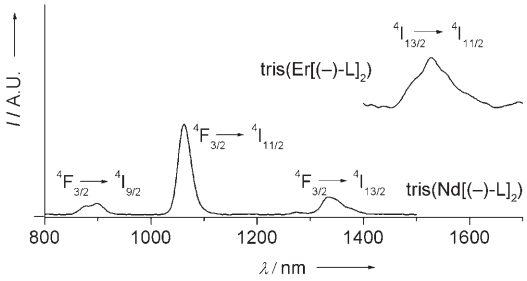

Figure 10. Normalized emission spectra in the NIR region of the tris(Nd[(−)-L]$_2$) and tris(Er[(−)-L]$_2$) complexes (CH_2Cl_2, λ_{ex} = 275 nm, RT).

Chiroptical properties: Solutions of the diprotonated (H_2L^+), neutral (H_2L), or anionic (L^-) forms of the enantiopure (+)- and (−)-L ligands show negligible CD activity in the range 230–500 nm, in accordance with reports of other pinene bipyridine ligands.[49] In contrast, a strong activity is displayed by solutions of all the tris(Ln[(+)-L]$_2$) or tris(Ln[(−)-L]$_2$) complexes in CH_2Cl_2 (Figure 11). The spectra are dominated by two bands centered around 309 and 280 nm that arise corresponding to the absorption maxima relative to the $\pi \rightarrow \pi^*$ transitions of the bipyridine moiety. Perfect mirror image spectra are recorded for the compounds containing the same metal ion and opposite enantiomers of the ligand, which is evidence for their supramolecular enantiomeric relationship (Figure 12). When the (+)-enantiomer of the ligand is employed, the most intense band (at 309 nm) assumes a negative sign ($\Delta\varepsilon \approx -100\,M^{-1}cm^{-1}$), whereas the most intense band at higher energies (280 nm) is positive ($\Delta\varepsilon \approx +30\,M^{-1}cm^{-1}$) and is split into two components. These bands, slightly shifted, are progressively diminishing in intensity in the complexes with the latter metals of the series (Dy, Ho, Er), thus going from Dy^{III} ($\Delta\varepsilon^{309} \approx -92\,M^{-1}cm^{-1}$) to Er^{III} ($\Delta\varepsilon^{311} \approx -62\,M^{-1}cm^{-1}$) complexes. This behavior could be a direct consequence of

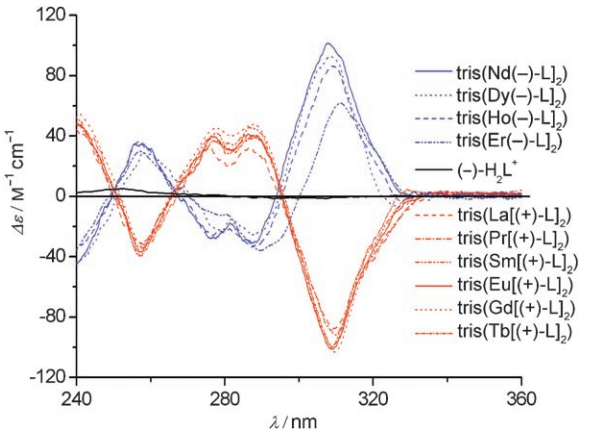

Figure 11. CD spectra of the ligand $(-)$-H_2L^+ and enantiopure tris(Ln[L]$_2$) complexes (CH_2Cl_2, 20 °C, $c \approx 1\times10^{-4}$ M).

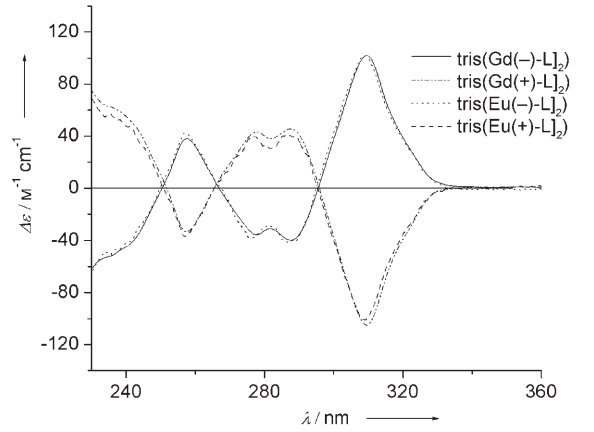

Figure 12. CD spectra of the enantiomeric pair of the tris(Ln[L]$_2$) complexes (Ln^{III} = Gd and Eu, CH_2Cl_2, 20 °C, $c = 1\times10^{-4}$ M).

slight structural distortions as a result of the decreased size of the metal ions.[50] The helical wrapping of the ligands around a metal core rather than a metal center, such as in the classical mononuclear complexes, defines a new version of supramolecular helical chirality, which is expressed by the strong Cotton effect observed, in the case of tris(Ln[L]$_2$) compounds. As discussed before, the two sets of ligands are individuating two distinct helical domains with opposite configurations. In terms of internuclear exciton coupling interactions,[50,51] only the set **S** should contribute to the CD activity. The three ligands of this set are in fact tightly bound to the Ln^{III} ions by both carboxylic and bipyridinic coordination sites. Therefore, they maintain a fixed mutual orientation. Instead, the contribution of set **S′**, in which the bipyridyl chromophores are uncoordinated thus free to rotate, should be negligible.

Consequently, a left-handed arrangement of set **S**, as in the case of the trinuclear structures obtained with (+)-L$^-$, should give rise to a bisignate curve positive at lower energies. The experimental curves (negative band at 309 nm) do not verify this prediction of exciton couplet theory.[52] Thus, besides the internuclear exciton couplings, other types of interactions are certainly involved.[53] The bipyridyl chromophores in set **S′** are uncoordinated and hence free to rotate; however, the contribution from set **S′** may not be as negligible as one may think from the conformational flexibility.

For the visible emitting complexes tris(Eu[(+)-L]$_2$) and tris(Tb[(+)-L]$_2$), additional spectroscopic information is provided by CPL spectroscopy. This technique is the emission analogue of CD and probes the chirality of the metal-centered excited states. When the Ln^{III} ion lies in a chiral environment, the magnitude of the dissymmetry factor quantifies the degree of chirality sensed by an electronic transition.[54] If in CD the dissymmetry factor is defined by Equation (1):

$$g_{abs} = \Delta\varepsilon/\varepsilon \quad (1)$$

in CPL measurements it follows from Equations (2a–c):

$$g_{em} = \Delta I/I \quad (2a)$$

$$\Delta I = I_L - I_R \quad (2b)$$

$$I = (I_L + I_R)/2 \quad (2c)$$

where I_L (and I_R) is the intensity of the left (or right) circularly polarized component of the luminescence. This leads to Equation (3):

$$g_{em} = 2(I_L - I_R)/(I_L + I_R) \quad (3)$$

Excitation of the organic chromophore (λ_{ex} = 315 nm) of the tris(Eu[(+)-L]$_2$) complex gives rise to polarized emission bands that correspond to the Eu^{III}-centered $^5D_0 \rightarrow {}^7F_J$ transitions. The largest dissymmetry factors are detectable in correspondence to transitions $^5D_0 \rightarrow {}^7F_1$ and $^5D_0 \rightarrow {}^7F_2$, with the first being more sensitive to the chiral environment and thus displaying an absolute value of $g_{em}(^5D_0 \rightarrow {}^7F_1)$ larger than $g_{em}(^5D_0 \rightarrow {}^7F_2)$. As in the case of CD, complexes synthesized from both the enantiomers of the ligand HL give rise to mirror image spectra (Figure 13). In the case of the tris(Tb[(+)-L]$_2$) complex, the largest dissymmetry factors are observed for $^5D_4 \rightarrow {}^7F_6$ and $^5D_4 \rightarrow {}^7F_5$ transitions with the latter expressing a larger g_{em} value (Figure 14).

The trinuclear complexes presented herein exhibit larger dissymmetric factors than other mononuclear Eu^{III} and Tb^{III} complexes obtained with bis(pinene terpyridine)[21] or tetraazacyclododecane-*N*,*N*′,*N*,*N*′-tetraacetic acid (DOTA)-type ligands.[55] Comparable g_{em} values for the transitions $\Delta J = 1$ and $\Delta J = 2$ are instead reported for Eu^{III} complexes with diethylene triamine pentaacetic acid (DTPA)[56] and DOTA[57] derivatives. A correlation between the overall helical chirality and the sign and intensity of the CPL transitions has not been well established.[58] Indeed most of the studies are based on the comparison among CPL spectra of structurally similar molecules whose configurations were previously determined in the solid state by X-ray diffraction studies.

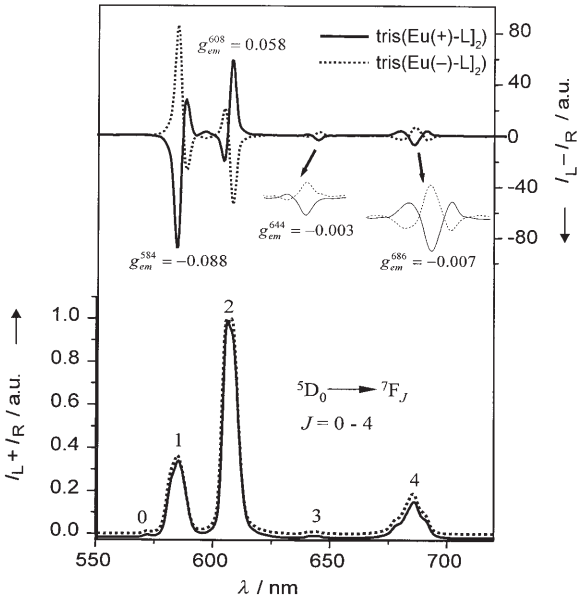

Figure 13. Total luminescence and CPL spectra for the two enantiomers tris(Eu[(+)-L]$_2$) and tris(Eu[(−)-L]$_2$) (CH_2Cl_2, $c = 1 \times 10^{-4}$ M, RT). The g_{em} values are given for the tris(Eu[(+)-L]$_2$) enantiomer.

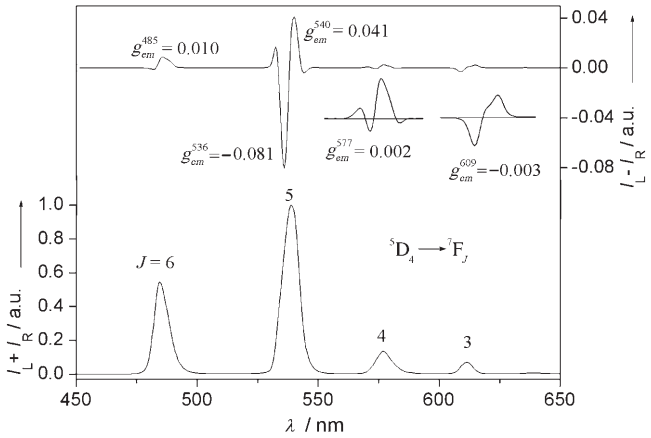

Figure 14. Total luminescence and CPL spectra of tris([Tb(+)-L]$_2$) (CH_2Cl_2, $c = 1 \times 10^{-4}$ M, RT).

Chiral recognition: Potential chiral discrimination phenomena were investigated by employing different enantiomeric mixtures of the ligand (i.e., (+)/(−) = 9:1, 7:3, 1:1) in the synthesis of trinuclear structures. The purpose of the presented study is to determine if a chiral-recognition process is actually involved in the self-assembly and, in this case, to establish whether homo- or heterorecognition takes place. Homorecognition refers to a chiral self-recognition process, in which the enantiomers of the ligand do not mix upon complexation; thus, solely discrete homochiral, enantiomeric architectures are obtained.[59–63] Conversely, heterorecognition is the result of a self-discrimination phenomenon from which a heterochiral self-assembled structure, containing both the enantiomers of the ligand, is afforded.[64–66]

In the present case, the self-assembly in methanol was performed with enantiomeric mixtures of ligand L^- and [Ln-$(ClO_4)_3$]·$x H_2O$ salts (Ln^{III} = La, Pr, Eu; metal/ligand = 1:2) and led, as in the case of the enantiopure ligand, to the virtually quantitative formation of a precipitate. The elemental analyses matched the calculated values for [$Ln_3L_6(\mu_3$-OH)-$(H_2O)_3$]$(ClO_4)_2$·$x H_2O$ in all cases. The other analyses (ES-MS, IR, UV) display similar results to those reported for the enantiopure tris(Ln[L]$_2$) species.

Moreover, the fact that the signals of the NMR spectra are superimposable on those that correspond to enantiopure complexes clearly demonstrates that mixtures of homochiral enantiomeric tris(Ln[L]$_2$) species are obtained. Nevertheless, some sets of unassigned side peaks are detected in low amounts (≈10%) regardless of the Ln ion used. This behavior proves that the self-assembly is slightly perturbed as a consequence of errors during the self-recognition process.

The CD spectra of these enantiomeric mixtures display an optical activity proportional to the excess of one enantiomer of the ligand over the other, namely, the enantiomeric excess (*ee*). Indeed, the experimental CD profiles of 9:1 and 7:3 samples closely follow the corresponding calculated profiles for a given enantiomeric excess (Figure 15). As an example, the Eu^{III} complex synthesized from a 7:3 mixture of (+) and (−)-L^- displays $\Delta\varepsilon^{308} = -42\,M^{-1}cm^{-1}$, which is about 40% of the value obtained with a solution of enantiopure tris(Eu[(+)-L]$_2$) complex ($\Delta\varepsilon^{308} = -101\,M^{-1}cm^{-1}$). This result indicates that 70% of the mixture presents the helical orientation (and CD activity) of tris(Eu[(+)-L]$_2$), whereas the remaining 30% is constituted by the enantiomer tris(Eu[(−)-L]$_2$). The resulting CD activity thus corresponds to 40% *ee* of the homochiral complex containing only the (+)-L enantiomer. Similarly, the sample obtained from the (+)/(−) = 9:1 mixture of ligands presents $\Delta\varepsilon^{308} = -83\,M^{-1}cm^{-1}$, thus

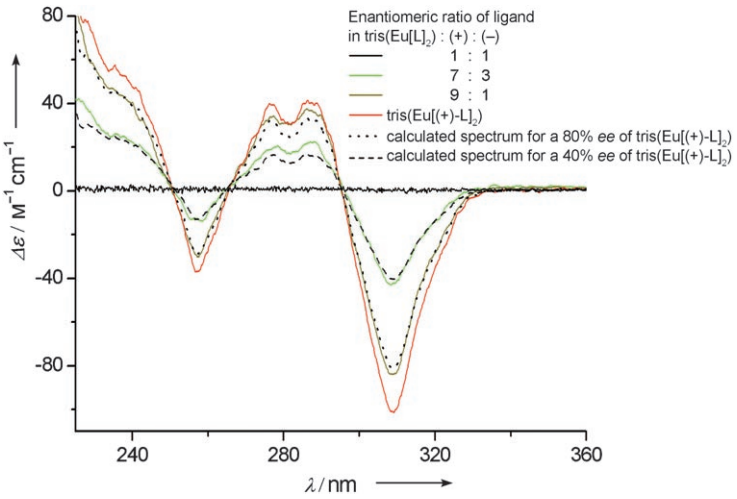

Figure 15. Experimental (solid lines, CH_2Cl_2, $c \approx 1 \times 10^{-4}$ M) and calculated (dotted lines) CD spectra of tris(Eu[L]$_2$) complexes synthesized from different enantiomeric mixtures of the ligand. The calculated curves are obtained by adding the two experimental CD profiles of the enantiopure complexes, which were previously multiplied by the percentage of the corresponding enantiomer.

corresponding to 80% of that given by the enantiopure tris(Eu[(+)-L]$_2$) sample, thus with a 80% *ee* of tris(Eu[(+)-L]$_2$) species. A spectrum void of signals is registered when a racemic mixture of the ligand was employed. All these data lead to the conclusion that a given initial enantiomeric excess of the ligand is conserved upon the self-assembly process, thus leading to a mixture of homochiral trinuclear species with the same enantiomeric excess.

A definitive proof of homochiral recognition was provided by X-ray analysis. Many attempts to crystallize the racemic mixture of trinuclear complexes containing the perchlorate counterion failed. This result prompted us to attempt the crystallization with other counterions (i.e., nitrate and triflate). High-quality crystals were grown by slow evaporation of an solution of raw material in acetonitrile, obtained by mixing an artificial racemic mixture of the ligand and the $Eu(CF_3SO_3)_3{\cdot}2H_2O$ salt. The complex crystallized as a racemate in the centrosymmetric triclinic space group $P\bar{1}$, containing the two enantiomers of general formula $[Eu_3(L)_6(OH)(H_2O)_3](CF_3SO_3)(Cl){\cdot}3H_2O{\cdot}8CH_3CN$ (Figure 16). As the reaction mixture was crystallized without any previous purification, the Cl^- ion (from the acidic (±)-HL·HCl) is present as a counterion. Each enantiomeric trinuclear structure is homochiral and isostructural with the one obtained from the enantiopure ligand. Thus the (+)-L isomer builds up a trinuclear species in which the two sets **S** and **S′** display *M*- and *P*-helical arrangements, respectively. Conversely, the mirror-image complex of the (−)-L^- enantiomer exhibits the opposite configuration (the *P* helix for set **S** and *M* helix for set **S′**).

A deeper structural investigation showed that relative to the enantiopure structures, the racemic trinuclear cations do not possess a C_3 axis. Indeed every metal center displays similar but nonetheless distinct coordination spheres in terms of bond lengths and angles. The distance of the μ_3-OH group from the plane formed by the three metal ions, and the coordination bonds, are in general found to be slightly larger in the racemic triflate structure relative to the enantiopure perchlorate complex (Table 2). The uncoordinated bipyridine moieties of ligands from set **S′** are found to adopt a *transoid* conformation, with dihedral angles of 162–144° (Table 3). In the present case, the hydrogen-bonding network, including the water molecules of crystallization, does not stabilize the *cis* conformation, as in the case of the enantiopure complexes. This behavior results because the water molecules are involved in a hydrogen-bonding network with the counterions (Cl^- and $CF_3SO_3^-$) and not with the nitrogen atoms from the bipyridine unit (Figure 17). Another interesting feature of the racemate structure is the intermolecular π–π interactions between two bipyridine moieties of set **S** that belong to the two enantiomeric complex molecules (Figure 18).

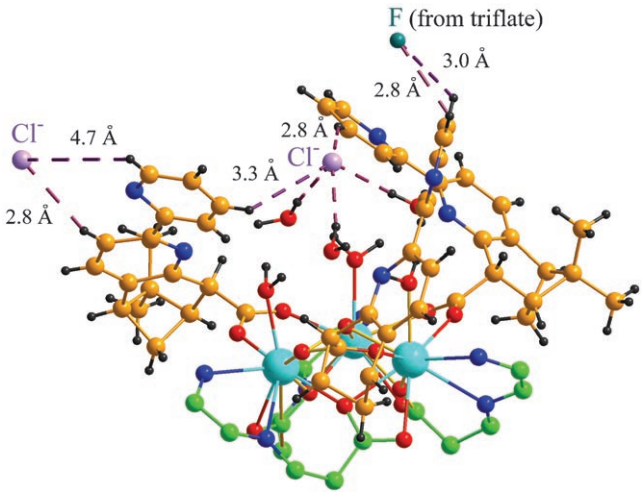

Figure 17. The hydrogen-bonding interactions in the X-ray structure of $[Eu_3\{(\pm)\text{-}L\}_6(OH)(H_2O)_3](CF_3SO_3)(Cl)$ involving the pyridine hydrogen atoms of ligands belonging to set **S′** (orange), Cl^- ions (purple), and fluorine atoms from $CF_3SO_3^-$ (dark green). For the sake of clarity, only the binding sites of the ligands of set **S** are presented.

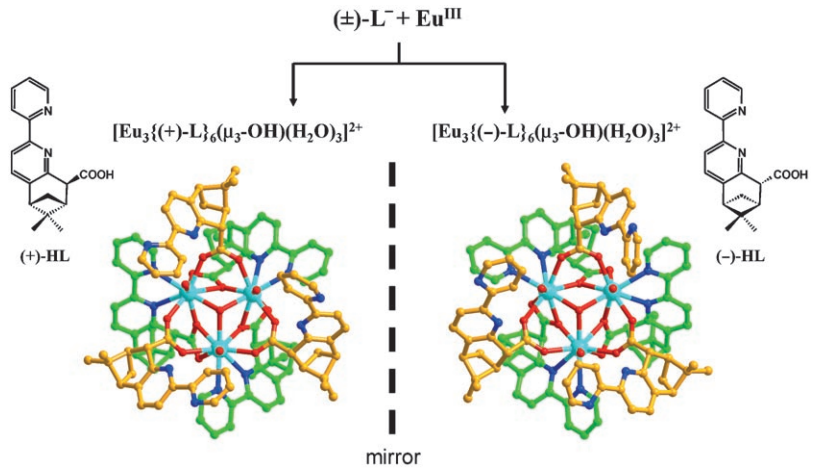

Figure 16. Representation of the chiral homorecognition process that leads to two enantiomeric complexes in the racemic crystal tris(Eu[(±)-L]$_2$). Eu: turquoise, N: blue, O: red, ligand set **S**: light green, ligand set **S′**: orange.

Conclusion

Herein, we have reported the diastereoselective synthesis of a self-assembled, enantiopure class of trinuclear, lanthanide-containing arrays. X-ray structural determinations were achieved for all the synthesized compounds, thus proving their isostructurality. A thorough spectroscopic characterization of the species in solution (^{1}H and ^{13}C NMR, ES-MS) led unequivocally to the conclusion that the trinuclear architecture is retained in weakly coordinating solvents, such as CH_2Cl_2.

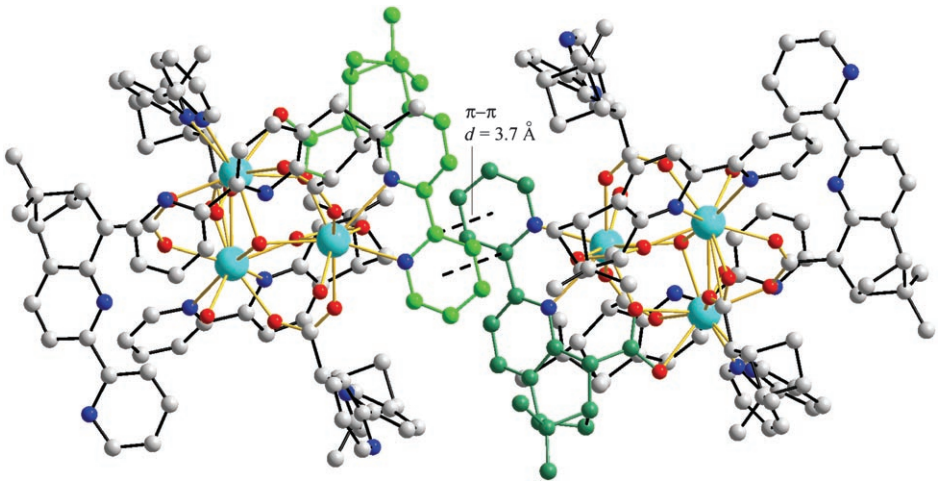

Figure 18. X-ray structure of the racemate $[Eu_3\{(\pm)\text{-}L\}_6(OH)(H_2O)_3](CF_3SO_3)(Cl)$ showing the two ligands involved in the intermolecular π–π interactions.

The arrangement of the ligands around the trimetallic core in two helical domains with opposite configurations accounts for an original version of supramolecular helical chirality. This behavior gave rise to a strong optical activity, as determined by CD and CPL spectroscopic analysis. Moreover some tris(Ln[L]$_2$) compounds displayed interesting emission properties in the visible (Ln^{III} = Eu and Tb) and NIR (Ln^{III} = Er and Nd) regions, thus proving that the ligand L^- is a good sensitizer for the lanthanide ions. These systems showed a strong aptitude for chiral self-recognition, as indicated by solution (^{1}H NMR, ES-MS, and CD) and X-ray (tris(Eu[(±)-L]$_2$) studies on compounds obtained from different enantiomeric mixtures of the ligand. The successful application of the pinene-based strategy in the synthesis of chirally predetermined Ln^{III}-containing arrays opens interesting possibilities for the development of new supramolecular asymmetric catalysts or magnetic resonance imaging (MRI) relaxation agents.

Experimental Section

Materials and analytical methods: Water-sensitive reactions were carried out in an inert atmosphere of argon in oven-dried glassware. Unless otherwise stated, commercial-grade solvents previously dried and deoxygenated by a solvent purification system based on alumina columns (Innov-Tech) were employed in the syntheses of the ligands and complexes. 2-Acetylpyridine (>98%) and α-pinene (99%, 97% *ee*) were purchased from Fluka and Aldrich, respectively. The Ln^{III} perchlorate salts were prepared from the corresponding oxides according to a previous procedure.[67] (**Caution**! Perchlorate salts are potentially explosive).[68,69] The concentrations of the stock solutions of $Ln(ClO_4)_3{\cdot}xH_2O$ in methanol were determined by complexometric titrations with $Na_2(H_2EDTA)$ (EDTA = ethylenediaminetetraacetic acid) and xylene orange as the indicator.

The X-ray diffraction data were collected on an Oxford Diffraction CrysAlis CCD at 140(2) K and on a Stoe Mark II-IPDS at 173(2) K. The structures were solved by direct methods using SHEXLS-97[70] and refined by the full-matrix least-squares method on F^2 using SHELXL-97.[71] Hydrogen atoms were included in calculated positions and treated as riding atoms. Multiscan absorption corrections were applied for the complexes. CCDC-637652 ((+)-HL-HCl), -637653 (tris(La[(−)-L]$_2$)), -607511 (tris(Pr[(+)-L]$_2$)), -637654 (tris(Nd-[(−)-L]$_2$)), -637655 (tris(Sm[(+)-L]$_2$)), -259970 (tris(Eu[(+)-L]$_2$)), -637656 (tris(Gd[(+)-L]$_2$)), -637657 (tris-(Tb[(+)-L]$_2$)), -637658 (tris(Dy[(−)-L]$_2$)), -637659 (tris(Eu[(±)-L]$_2$)), -637660 (tris(Ho[(−)-L]$_2$)), and -637661 (tris(Er[(−)-L]$_2$) contain the supplementary data for this paper. These data can be obtained free of charge from the Cambridge Crystallographic Data Centre via www.ccdc.cam.ac.uk/data_request/cif.

IR spectra were collected in the range 4000–550 cm^{-1} with a Perkin-Elmer FT-IR Spectrum One provided with an ATR sampling accessory. ES mass spectra were obtained with an instrument LCT from Waters-Micromass, combining an ES source and a time-of-flight (TOF) analyzer. Solutions of the metal complexes were diluted to 10^{-4}, 10^{-5}, and 10^{-6} M and injected by infusion at a flow rate of 5 μL min^{-1}. The ion-spray voltage was set at 2600 and 12 V for the sample cone, and the source temperature was 120 °C. The spectra are the averaged result of a 1-min scan from m/z 200–2500 at a rate of 1 scan s^{-1}. Deconvolution was performed using Masslynx 3.4 software. Theoretical isotopic distribution was calculated by using the software ChemCalc.[72] ^{1}H and ^{13}C NMR spectra were registered on Bruker Avance 400 (400 MHz) and Bruker Avance 600 (600 MHz) spectrometers. The chemical shift values are referenced to the trimethylsilane (TMS) standard (δ = 0 ppm), whereas the residual proton impurities of CD_2Cl_2 was used as the internal reference.

Spectrophotometric measurements: Suprasil quartz cells and spectrophotometric grade solvents (CH_2Cl_2) were employed. The measurements at low temperature (77 K) were performed in quartz tubes inserted in a liquid-nitrogen-filled quartz dewar. UV/Vis spectra were recorded on Perkin-Elmer Lambda900 or Varian Cary 5000 double-beam UV/Vis/NIR spectrometers and baseline corrected. Steady-state luminescence emission spectra were recorded on a HORIBA Jobin-Yvon IBH FL-322 Fluorolog 3 spectrometer equipped with a 450-W xenon arc lamp. Steady-state NIR measurements were performed using the Fluorolog 3 spectrometer equipped with a peltier-cooled Hamamatsu H9170–75 (InP/InGaAs) PMT in the spectral range 930–1700 nm. Emission and excitation spectra were corrected in all the cases for source intensity (lamp and grating) and emission spectral response (detector and grating) by standard correction curves. The lifetimes of the europium and terbium complexes were recorded on the Fluorolog 3 spectrometer using the FL-1040 phosphorescence module with a 70-W xenon flash tube (full-width at half maximum (FWHM) = 3 μs) with a variable flash rate (0.05–25 Hz). The signals were recorded on the TBX-4-X single-photon-counting detector and collected with a multichannel scaling (MCS) card in the IBH DataStation Hub photon counting module, and data analysis was performed using the commercially available DAS6 software (HORIBA Jobin Yvon IBH). The goodness-of-fit was assessed by minimizing the reduced chi squared function (χ^2) and visual inspection of the weighted residuals. Time-resolved NIR measurements were measured on an FL900CDT time-resolved T-Geometry fluorometer equipped with a LTB MSG 400 nitrogen laser (337 nm; pulse energy = 20 μJ, repetition rate = 10 Hz) and a North Coast EO 817P liquid-nitrogen-cooled germanium detector with a time resolution of 0.3 μs. The signals were averaged using a digitized Tektronix oscilloscope and then analyzed using standard fitting software. Luminescence quantum yields (Φ_{em}) were measured on optically dilute solutions (absorbance value lower than 0.1 at excitation wavelength). Quantum yields for the Eu^{III} and Tb^{III} complexes were determined relative to those of $[Ru(2,2'\text{-bipyridine})_3]Cl_2$ (Φ_{em} = 1.6% in CH_3CN)[73] and

to quininie bisulfate ($\Phi_{em}=54.6\,\%$ in $1\,N$ H_2SO_4),[74] respectively. Quantum yields for the Nd^{III} and Er^{III} complexes were determined with respect to $[Yb(TTA)_3{\cdot}2H_2O]$ (TTA = (4-tolylsulfanyl)acetate) as a standard ($\Phi_{em}=0.35\,\%$ in toluene).[75] The estimated errors are $\pm 20\,\%$ for the quantum yields and $\pm 5\,\%$ for the lifetime determinations.

The CD spectra were recorded with a Jasco J-810 spectrometer. The solutions (CH_2Cl_2, $c=1\times10^{-4}$ M) were thermostated at 20.0 °C using a Jasco PFD-425S system.

The CPL spectra were measured using a Jasco CPL-200 spectrophotometer (CH_2Cl_2, $c=1\times10^{-4}$ M, RT, bandwidth = 2 nm, $\lambda_{ex}=320$ nm with a xenon lamp, scan rate = 20 nm min^{-1}, averaged over 12 scans).

Synthesis of the ligands and complexes

Precursors: Both enantiomers of 5,6-pinene bipyridine were synthesized from (−)- or (+)-α-pinene, according to a reported procedure.[28]

Preparation of (+)-HL·HCl: In an inert atmosphere, dry THF (30 mL) was cooled down to −20 °C in a double-necked round-bottomed flask. Freshly distilled LDA (0.75 mL, 5.3 mmol) was added to the solution, followed by n-BuLi (2 mL, 2.5 M in hexane, 5 mmol). The solution was warmed to 0 °C for 10 min and successively cooled down to −40 °C. A solution of (−)-5,6-pinene-bipyridine (1 g, 4 mmol) in THF (15 mL) was then added dropwise over 30 min. The dark blue solution obtained was stirred at −40 °C for 2 h. Dried, gaseous CO_2 was then bubbled until decoloration. After warming up to room temperature, the excess of base was quenched with water (0.3 mL). The solvent was evaporated, and the crude reaction mixture was first dissolved in CH_2Cl_2 and then extracted with water (3 × 20 mL). The collected aqueous fractions were acidified (pH 1.5–2) with HCl 35 %, and the water was removed by evaporation under reduced pressure. The resulting solid compound was washed with cold CH_3CN and CH_2Cl_2 and dried to yield 980 mg (70 %) of product. The analyses are similar to those reported by us previously.[26]

Deprotonation of (+)-HL·HCl (15 mg, 0.04 mmol) was performed in CD_2Cl_2 by addition of TEA (18 μL, 0.096 mmol, 2.4 equiv). ^{1}H NMR (400 MHz, CD_2Cl_2, 25 °C): $\delta=8.64$ (d, $J_{1,2}=5.8$ Hz, 1H, H(1)), 8.37 (d, $J_{4,3}=8.0$ Hz, 1H, H(4)) = 8.13 (d, 2H, $J_{7,8}=7.9$ Hz, 1H, H(7)), 7.78 (dd, $J_{3,4}=8.0$ Hz, $J_{3,2}=6.5$ Hz, 1H, H(3)), 7.38 (d, $J_{8,7}=7.9$ Hz, 1H, H(8)), 7.27 (dd, $J_{2,3}=6.5$ Hz, $J_{2,1}=5.8$ Hz, 1H, H(2)), 3.95 (d, $J_{13,12}=2.5$ Hz, 1H, H(13)), 2.99 (dd, $J_{10,15a}=5.6$ Hz, $J_{10,15b}=5.6$ Hz, 1H, H(10)), 2.91 (ddt, $J_{12,15b}=5.8$ Hz, $J_{12,10}=5.8$ Hz, $J_{12,15b}=2.8$ Hz, 1H, H(12)), 2.74 (ddd, $J_{15b,15a}=9.6$ Hz, $J_{15b,10}=5.81$ Hz, $J_{15b,12}=5.81$ Hz, 1H, H(15b)), 1.88 (d, $J_{15a,15b}=9.6$ Hz, 1H, H(15a)), 1.47 (s, 3H, Me(17)), 0.69 ppm (s, 3H, Me(16)).

Preparation of (−)-HL·HCl: The reaction leading to (−)-HL was performed under the same conditions, with (+)-5,6-pinene bipyridine as the starting material. The yield and the analyses were similar to those obtained for the + isomer, except the $[\alpha]_D$ value which has the opposite sign, $[\alpha]_D^{20}=-13.7°\,dm^2\,mol^{-1}$ (589 nm; 7.1×10^{-3} M, CH_3CN).

General procedure for the preparation of $[Ln_3L_6(OH)(H_2O)_3](ClO_4)_2$ (tris(Ln[L]$_2$)): TEA (98 μL, 0.67 mmol, 2.3 equiv) was added to a solution of (+)- or (−)-HL·HCl·H_2O (100 mg, 29.5 mmol, 1 equiv) in methanol (3 mL). A solution of $Ln(ClO_4)_3{\cdot}xH_2O$ (about 0.05 M, 0.5 equiv) in methanol was then dropped into the stirred mixture. A white precipitate formed quantitatively, was collected by filtration, washed with cold methanol, and dried under high vacuum (10^{-5} mbar). Suitable crystals for X-ray analysis were grown by slow evaporation of the product in solution with CD_3CN.

$[La_3\{(+)\text{-}L\}_6(OH)(H_2O)_3](ClO_4)_2$: $[\alpha]_D^{20}=-158.2°\,dm^2\,mol^{-1}$ (589 nm, 5.8×10^{-3} M, CH_2Cl_2); CD (λ [nm] ($\Delta\varepsilon$)) = 309 (−87), 287 (32), 276 (32); ^{1}H NMR (400 MHz, CD_2Cl_2, 20 °C): $\delta=8.67$ (d, $J_{1',2'}=4.8$ Hz, 1H, H(1′)), 8.40 (d, $J_{4',3'}=8.0$ Hz, 1H, H(4′)), 8.26 (d, $J_{7',8'}=7.9$ Hz, 1H, H(7′)), 7.98 (m, 3H, H(3′), H(4) and H(7)), 7.89 (ddd, $J_{3,2}=6.8$ Hz, $J_{3,4}=6.8$ Hz, $J_{3,1}=1.7$ Hz, 1H, H(3)), 7.70 (d, $J_{1,2}=5.1$ Hz, 1H, H(1)), 7.63 (d, $J_{8,7}=8.1$ Hz, 1H, H(8)), 7.56 (d, $J_{8',7'}=7.8$ Hz, 1H, H(8′)), 7.30 (dd, $J_{2',3'}=6.6$ Hz, $J_{2',1'}=6.6$, 1H, H(2′)), 6.89 (d, $J_{2,3}=6.8$ Hz, $J_{2,1}=6.6$, 1H, H(2)), 4.07 (d, $J_{13,12}=2.1$ Hz, 1H, H(13)), 3.56 (d, $J_{13',12'}=2.4$ Hz, 1H, H(13′)), 2.95 (dd, $J_{10,15b}=5.6$ Hz, $J_{10,12}=5.6$, 1H, H(10)), 2.75 (dd, $J_{10',15b'}=5.7$ Hz, $J_{10',12'}=5.7$, 1H, H(10′)), 2.70 (ddd, $J_{15b,15a}=9.6$ Hz, $J_{15b,10}=5.5$ Hz, $J_{15b,12}=5.5$ Hz, 1H, H-(15b)), 2.53 (ddd, $J_{12,15b}=5.7$ Hz, $J_{12,15b}=5.7$ Hz, $J_{12,10}=2.5$ Hz, 1H, H(12)), 2.03 (ddd, $J_{15b,15a}=9.6$ Hz, $J_{15b,10}=5.6$ Hz, $J_{15b,12}=5.6$ Hz, 1H, H-(15b′)), 1.44 (m, 2H, H(15a), H(15a′)), 1.41 (s, 3H, Me 17), 1.27 (s, 3H, Me 17′), 1.06 (ddd, $J_{12',15b'}=5.7$ Hz, $J_{12',15b'}=5.7$ Hz, $J_{12',10'}=2.5$ Hz, 1H, H-(12′)), 0.53 (s, 3H, Me 16), 0.48 ppm (s, 3H, Me 16′); ^{13}C NMR (100 MHz, CD_2Cl_2, 20 °C): $\delta=181.7$, 180.5, 156.7, 156.4, 155.8 (2C), 154.8, 153.2, 149.9, 148.8, 146.5, 142.9, 140.3, 138.2, 137.0, 135.0, 125.1, 124.2, 123.6, 121.9, 121.6, 119.5, 53.2, 51.8, 46.7 (2C), 44.3, 42.8, 41.0, 31.9, 29.2, 26.0, 25.7, 21.1, 21.0, 11.7 ppm; IR: $\tilde{\nu}=2935$w (ν(C–H) aliphatic), 1608 s (ν_{as} (COO^-)), 1566 m, 1453w, 1416s (ν_s (COO^-)), 1239w, 1094s (ν(Cl–O)), 860w, 792m, 754m cm^{-1}; UV/Vis (λ [nm] (ε [M^{-1}cm^{-1}])) = 303 (79 000), 255 (58 000); ES-MS (10^{-4} M in CH_2Cl_2): *m/z*: 2293.34 (100) $[La_3L_6(OH)+(ClO_4)]^+$, 1096.58 (50) $[La_3L_6(OH)]^{2+}$; elemental analysis calcd (%) for $C_{108}H_{109}La_3N_{12}O_{24}Cl_2{\cdot}5H_2O$: C 51.13, H 4.73, N 6.63; found: C 51.21, H 4.64, N 6.56.

$[Pr_3\{(+)\text{-}L\}_6(OH)(H_2O)_3](ClO_4)_2$: $[\alpha]_D^{20}=-169°\,dm^2\,mol^{-1}$ (589 nm, 5.8×10^{-3} M, CH_2Cl_2); CD (λ [nm] ($\Delta\varepsilon$)) = 310 (−95), 288 (40), 277 (38); ^{1}H NMR (400 MHz, CD_2Cl_2, 20 °C): $\delta=27.52$ (bs, 1H, H(15a′)), 26.24 (bs, 1H, H(12′)), 21.03 (bs, 1H, H(13) or (13′)), 19.20 (bs, 1H, H(13′)or (13)), 15.42 (bs, 1H, H(15b′)), 12.43 (d, $J_{8,7}=7.6$ Hz, 1H, H(8)), 12.20 (bs, 1H, H(15a)), 11.36 (d, $J_{8',7}=8.1$ Hz, 1H, H(8′)), 11.26 (d, $J_{7,8}=7.6$ Hz, 1H, H(7)), 9.59 (bs, 1H, H(10′)), 9.28 (d, $J_{7',8'}=8.2$ Hz, 1H, H(7′)), 7.62 (s, 3H, Me 17′), 7.41 (bs, 1H, H(4)), 7.16 (bs, 1H, H(2)), 6.98 (bs, 1H, H(3)), 6.14 (bs, 1H, H(10)), 6.05 (s, 3H, Me 16′), 4.20 (bs, 1H, H(2′) or H(3′)), 4.01 (bs, 1H, H(15b)), 3.43 (bs, 1H, H(1′) or H(4′)), 3.05 (bs, 1H, H(3′) or (H2′)), 3.04 (bs, 1H, H(4′) or H(1′)), −0.35 (s, 3H, Me 17), −3.97 (s, 3H, Me 16), −4.61 (bs, 1H, H(12)), −11.10 ppm (bs, 1H, H(1)); ^{13}C NMR (100 MHz, CD_2Cl_2, 20 °C): $\delta=250.5$, 174.0, 169.8, 161.4, 157.0, 155.1, 154.4, 153.1, 152.4, 146.5, 141.7, 140.8, 137.6, 134.1, 133.2, 131.4, 130.5, 127.1, 122.3, 120.7, 116.3, 77.2, 65.2, 64.4, 58.0, 54.7, 51.6, 40.7, 39.9, 36.8, 33.2, 30.2, 27.9, 24.3, 17.7, 1.2 ppm; IR: $\tilde{\nu}=2935$w (ν(C–H) aliphatic), 1610 s ($\nu_{as}(COO^-)$), 1567m, 1454w, 1419s ($\nu_s(COO^-)$), 1240w, 1095s (ν(Cl–O)), 860w, 792m, 754m, 622m; UV/Vis (λ [nm] (ε [M^{-1}cm^{-1}])): 303 (79 000), 255 nm (59 000); ES-MS (10^{-4} M in CH_2Cl_2): *m/z*: 2298.87 (100) $[Pr_3L_6(OH)+(ClO_4)]^+$, 1099.90 (20) $[Pr_3L_6(OH)]^{2+}$, 1090.90 (10) $[Pr_3(L)_6(OH)(H_2O)]^{2+}$; elemental analysis calcd (%) for $C_{108}H_{109}Pr_3N_{12}O_{24}Cl_2{\cdot}3H_2O$: C 51.75, H 4.62, N 6.71; found: C 51.62, H 4.35, N 6.43.

$[Nd_3\{(-)\text{-}L\}_6(OH)(H_2O)_3](ClO_4)_2$: $[\alpha]_D^{20}=171.3°\,dm^2\,mol^{-1}$ (589 nm, 5.8×10^{-3} M, CH_2Cl_2); CD (λ [nm] ($\Delta\varepsilon$)): 308 (101), 287 (−31), 276 (−27); ^{1}H NMR (400 MHz, CD_2Cl_2, 20 °C): $\delta=23.76$ (bs, 1H, H(13 or 13′), 12.77(bs, 1H, H(15a′)), 10.66 (bs, 1H, H(12′)), 10.15 (bs, 1H, H(2) or H(4)), 10.01 (bd, $J=5.9$ Hz, 1H, H(4) or H(2)), 9.96 (bd, $J_{7,8}=6.1$ Hz, 1H, H(7′)), 9.90 (bs, 1H, H(13 or 13′), 9.75 (d, $J_{8,7}=7.6$ Hz, 1H, H(8)), 9.33 (bs, 1H, H(3)), 9.27 (bs, 2H, H(8′) and H(7)), 7.45 (bs, 1H, H(15b′)), 6.93 (bs, 1H, H(1′ or 4′)), 5.93 (bs, 1H, H(10′)), 5.50 (bs, 2H, (15a) and H(4′ or 1′)), 4.36 (bs, 1H, H(2′ or 3′)), 4.02 (bs, 1H, H(10)), 3.96 (bs, 1H, H(3′ or 2′)), 3.75 (s, 3H, Me17′), 2.67 (bs, 1H, H(15b)), 2.52 (s, 3H, Me16′), 0.23 (s, 3H, Me17), −1.38 (bs, 1H, H(12)), −2.32 (s, 3H, Me16), −5.63 ppm (bs, 1H, H(1)); ^{13}C NMR (100 MHz, CD_2Cl_2, 20 °C): $\delta=$ 194.5, 164.0, 158.8, 157.4, 155.7, 154.5, 153.9, 153.3, 148.8, 147.6, 141.7, 140.6, 138.7, 138.0, 136.1, 136.0, 135.3, 131.3, 122.2, 121.5, 119.6, 111.2, 80.8, 51.2, 48.7, 48.4, 48.2, 39.8, 39.3, 36.6, 32.4, 28.7, 24.4, 23.7, 18.6, 1.12 ppm; IR: $\tilde{\nu}=2935$w (ν(C-H) aliphatic), 1611s ($\nu_{as}COO^-$)), 1567m, 1454w, 1420s ($\nu_s(COO^-)$), 1233w, 1095s (ν(Cl–O)), 860w, 792m, 754m, 622m cm^{-1}; UV/Vis (λ [nm] (ε, M^{-1}cm^{-1}])): 304 (79 000), 255 (56 000); ES-MS (10^{-4} M in CH_2Cl_2): *m/z*: 2307.82 (100) $[Nd_3L_6(OH)+(ClO_4)]^+$, 1104.41 (40) $[Nd_3L_6(OH)]^{2+}$, 1094.88 (10) $[Nd_3L_6(OH)(H_2O)]^{2+}$; elemental analysis calcd (%) for $C_{108}H_{109}Nd_3N_{12}O_{24}Cl_2{\cdot}H_2O$: C 52.29, H 4.51, N 6.78; found: C 52.55, H 4.13, N 6.74.

$[Sm_3\{(+)\text{-}L\}_6(OH)(H_2O)_3](ClO_4)_2$: $[\alpha]_D^{20}=-170.6°\,dm^2\,mol^{-1}$ (589 nm, 5.8×10^{-3} M, CH_2Cl_2); CD (λ [nm] ($\Delta\varepsilon$)): 309(−100), 287(45), 278(42); ^{1}H NMR (400 MHz, CD_2Cl_2, 20 °C): $\delta=10.48$ (bs, 1H, H(1)), 8.47 (d, $J_{7',8'}=7.9$ Hz, 1H, H(7′)), 8.40 (d, $J_{7,8}=8.0$ Hz, 1H, H(7)), 8.33 (d, $J_{1',2'}=4.0$ Hz, 1H, H(1′)), 8.27 (d, $J_{4,3}=8.1$ Hz, 1H, H(4)), 8.12 (dd, $J_{3,2}=7.5$ Hz, $J_{3,4}=7.5$ Hz, 1H, H(3)), 7.90 (m, 2H, H(8) and H(8′)), 7.45 (d, $J_{4',3'}=8.0$ Hz, 1H, H(4′)), 7.29 (m, 2H, H(2) and H(3′)), 6.95 (dd, $J_{2',3'}=6.5$ Hz, $J_{2',1'}=6.5$, 1H, H(2′)), 4.51 (bs, 1H, H(13)), 3.27 (dd, $J_{10,15b}=5.2$ Hz, $J_{10,12}=5.2$, 1H, H(10)), 3.15 (d, $J_{15a,15b}=9.1$ Hz, 1H, H(15a)), 3.03 (dd,

$J_{10',15b'}=5.4$ Hz, $J_{10',12'}=5.4$, 1H, H(10′)), 2.92 (m, 2H, H(12) and H(15b)), 2.69 (bs, 1H, H(13′)), 2.57 (bs, 1H, H(15b′)), 1.92 (d, $J_{15a',15b'}=9.8$ Hz, 1H, H(15a′)), 1.74 (s, 3H, Me17), 1.73 (under Me 17 peak, 1H, H(12′)), 1.16 (s, 3H, Me 17′), 0.87 (s, 3H, Me 16), 0.00 ppm (s, 3H, Me 16′); ^{13}C NMR (100 MHz, CD_2Cl_2, 20 °C): $\delta=187.7$, 185.3, 157,1 (2C), 155.7, 155.2, 155.1, 154.1, 149.4, 146.3, 143.8, 140.7, 137.9, 137.2, 135.6, 125.1, 123.0, 121.4, 119.8, 50.1, 50.0, 47.5 (2C), 46.6 (2C), 46.0 (2C), 43.4, 40.6, 30.6, 26.4, 25.4, 21.5 (2C), 20.7, 20.6 ppm; IR: $\tilde{\nu}=2935$w (ν(C−H) aliphatic), 1614s (ν_{as} COO^-)), 1568m, 1455w, 1421s ($\nu_s(COO^-)$), 1239w, 1094s (ν(Cl−O)), 861w, 792 m, 754m, 622 m cm^{-1}; UV/vis (λ [nm] (ε, M^{-1}cm^{-1})): 303 (79000), 255 (56500); ES-MS (10^{-4}M in CH_2Cl_2): *m/z*: 1114.68 (100) $[Sm_3L_6(OH)]^{2+}$, 2327.62 (60) ($[Sm_3L_6(OH)+(ClO_4)]^+$; elemental analysis calcd (%) for $C_{108}H_{109}Sm_3N_{12}O_{24}Cl_2{\cdot}4H_2O$: C 50.81, H 4.62, N 6.58; found: C 50.86, H 4.57, N 6.60.

$[Eu_3\{(-)\text{-}L\}_6(OH)(H_2O)_3](ClO_4)_2$: $[\alpha]_D^{20}=169.0°$ dm^{2}mol^{-1} (589 nm, 5.8×10^{-3}M, CH_2Cl_2); CD (λ [nm] ($\Delta\varepsilon$)): 310 (101), 288 (−40), 277 (−39); ^{1}H NMR (400 MHz, CD_2Cl_2, 20 °C): $\delta=13.33$ (bs, 1H, H(1)), 11.69 (bs, 1H, H(1′)), 11.64 (d, $J_{4',3'}=6.0$ Hz, 1H, H(4′)), 10.99 (bs, 1H, H(3′)), 9.23 (dd, $J_{2',3'}=6.9$ Hz, $J_{2',1'}=5.0$, 1H, H(2′)), 7.33 (d, $J_{7',8'}=7.5$ Hz, 1H, H(7′)), 6.47 (dd, $J_{3,2}=6.7$ Hz, $J_{3,4}=6.7$ Hz, 1H, H(3)), 5.97 (1H, H(12)), 5.58 (d, $J_{8,7}=7.6$ Hz, 1H, H(8)), 5.49 (d, $J_{8',7'}=7.6$ Hz, 1H, H(8′)), 5.08 (d, $J_{7,8}=7.3$ Hz, 1H, H(7)), 4.57 (d, $J_{4,3}=6.7$ Hz, 1H, H(4)), 3.51 (s, 3H, Me 16), 3.23 (bd, $J_{2,3}=6.8$ Hz, 1H, H(2)), 3.05 (s, 1H, H(15b)), 2.55 (s, 3H, Me 17), 1.52 (bs, 1H, H(10)), −0.39 (bs, 1H, H(10′)), −1.73 (s, 3H, Me 17′), −2.20 (s, 3H, Me 16′), −2.27 (d, $J_{15a,15b}=$ −10.3 Hz, 1H, H(15a)), −3.44 (bs, 1H, H(15b′)), −5.40 (bs, 1H, H(13′)), −7.38 (bs, 1H, H(13)), −9.38 (bs, 1H, H(15a′)), −11.72 ppm (bs, 1H, H(12′)); ^{13}C NMR (100 MHz, CD_2Cl_2, 20 °C): $\delta=228.9$, 190.1, 169.5, 160.7, 156.8, 154.4, 152.9, 152.2, 151.0, 147.4, 146.5, 141.9, 140.3, 136.0, 132.0, 128.3, 126.3, 124.9, 117.8, 105.4, 104.3, 93.1, 45.5, 43.3, 42.7, 41.9, 35.8, 30.1, 26.5, 23.3, 23.0, 21.2, 18.0, 1.1, −8.9, −40.5 ppm; IR: $\tilde{\nu}=2935$w (ν(C−H) aliphatic), 1618s (ν_{as} (COO^-)), 1567m, 1454w, 1421s ($\nu_s(COO^-)$), 1238w, 1094s (ν(Cl−O)), 860w, 792m, 753m, 622m cm^{-1}; UV/Vis (λ [nm] (ε, M^{-1}cm^{-1})): 304 (79000), 255 (59000); ES-MS (10^{-4}M in CH_2Cl_2): *m/z*: 2331.58 (100) $[Eu_3L_6(OH)+(ClO_4)]^+$, 1116.34 (15) $[Eu_3(L)_6(OH)]^{2+}$, 1107.32 (<5) $[Eu_3(L)_6(OH)(H_2O)]^{2+}$; elemental analysis calcd (%) for $C_{108}H_{109}Eu_3N_{12}O_{24}Cl_2{\cdot}4H_2O$: C 50.71, H 4.61, N 6.57; found: C 50.84, H 4.33, N 6.32.

$[Gd_3\{(+)\text{-}L\}_6(OH)(H_2O)_3](ClO_4)_2$: $[\alpha]_D^{20}=-178.3°$ dm^{2}mol^{-1} (589 nm, 5.8×10^{-3}M, CH_2Cl_2); CD (λ [nm] ($\Delta\varepsilon$): 310 (−103), 288 (48), 278 (45); IR: $\tilde{\nu}=2935$w (ν(C−H) aliphatic), 1614s ($\nu_{as}(COO^-)$), 1567m, 1455w, 1422s ($\nu_s(COO^-)$), 1233w, 1094s (ν(Cl−O)), 863w, 792m, 753m, 622m cm^{-1}; UV/Vis (λ [nm] (ε [M^{-1}cm^{-1}])): 304 (80000), 255 (58000); ES-MS (10^{-4}M in CH_2Cl_2): *m/z* 2347.90 (100) $[Gd_3L_6(OH)+(ClO_4)]^+$, 1124.41 (50) $[Gd_3L_6(OH)]^{2+}$; elemental analysis calcd (%) for $C_{108}H_{109}Gd_3N_{12}O_{24}Cl_2{\cdot}3H_2O$: C 50.75, H 4.54, N 6.58; found: C 50.92, H 4.35, N 6.46.

$[Tb_3\{(+)\text{-}L\}_6(OH)(H_2O)_3](ClO_4)_2$: $[\alpha]_D^{20}=-163.8°$ dm^{2}mol^{-1} (589 nm, 5.8×10^{-3}M, CH_2Cl_2); CD (λ [nm] ($\Delta\varepsilon$): 309 (−100), 288 (41), 277 (37); IR: $\tilde{\nu}=2935$w (ν(C−H) aliphatic), 1615s ($\nu_{as}(COO^-)$), 1568m, 1455w, 1422s ($\nu_s(COO^-)$), 1234w, 1092s (ν(Cl−O)), 861w, 792 m, 753m, 622 m cm^{-1}; UV/Vis (λ [nm] (ε [M^{-1}cm^{-1}])): 303 (78000), 255 (58500); ES-MS (10^{-4}M in CH_2Cl_2): *m/z*: 2352.90 (100) ($[Tb_3(L)_6(OH)+(ClO_4)]^+$, 1126.91 (30) $[Nd_3(L)_6(OH)]^{2+}$; elemental analysis calcd (%) for $C_{108}H_{109}Tb_3N_{12}O_{24}Cl_2{\cdot}3H_2O$: C 50.65, H 4.53, N 6.56; found: C 50.66, H 4.36, N 6.37.

$[Dy_3\{(-)\text{-}L\}_6(OH)(H_2O)_3](ClO_4)_2$: $[\alpha]_D^{20}=163.4°$ dm^{2}mol^{-1} (589 nm, 5.8×10^{-3}M, CH_2Cl_2); CD (λ [nm] ($\Delta\varepsilon$)): 309(92), 288(−27), 279(−22); IR: $\tilde{\nu}=$ 2935w (ν(C−H) aliphatic), 1618s ($\nu_{as}(COO^-)$), 1568m, 1455w, 1422s (ν_s (COO^-)), 1234w, 1093s (ν(Cl−O)), 862w, 792m, 753m, 622m cm^{-1}; UV/Vis (λ [nm] (ε [M^{-1}cm^{-1}])): 303 (77000), 255 (58000); ES-MS (10^{-4}M in CH_2Cl_2): *m/z*: 1131.03 (100) $[Dy_3(L)_6(OH)]^{2+}$, 2359.08 (20) ($[Dy_3(L)_6(OH)+(ClO_4)]^+$; elemental analysis calcd (%) for $C_{108}H_{109}Dy_3N_{12}O_{24}Cl_2{\cdot}4H_2O$: C 50.09, H 4.55, N 6.49; found: C 49.84, H 4.52, N 6.64.

$[Ho_3\{(-)\text{-}L\}_6(OH)(H_2O)_3](ClO_4)_2$: $[\alpha]_D^{20}=156.7°$ dm^{2}mol^{-1} (589 nm, 5.8×10^{-3}M, CH_2Cl_2; CD (λ [nm] ($\Delta\varepsilon$)): 309(86), 287(33), 277(−27); IR: $\tilde{\nu}=$ 2935w (ν(C−H) aliphatic), 1618s ($\nu_{as}(COO^-)$), 1568m, 1456w, 1425s (ν_s (COO^-)), 1237w, 1093, 1081s (ν(Cl−O)), 862w, 792 m, 754m, 622m cm^{-1}; UV/Vis (λ [nm] (ε [M^{-1}cm^{-1}])): 304 (80000), 255 (58000); ES-MS (10^{-4}M in CH_2Cl_2): *m/z*: 1135.81 (100) $[Ho_3L_6(OH)]^{2+}$, 2369.46 (<5) $[Ho_3L_6(OH)+(ClO_4)]^+$; elemental analysis calcd (%) for $C_{108}H_{109}Ho_3N_{12}O_{24}Cl_2{\cdot}H_2O$: C 51.01, H 4.40, N 6.61; found: C 51.25, H 4.52, N 6.67.

$[Er_3\{(-)\text{-}L\}_6(OH)(H_2O)_3](ClO_4)_2$: $[\alpha]_D^{20}=148.4°$ dm^{2}mol^{-1} (589 nm, 5.8×10^{-3}M, CH_2Cl_2); CD (λ [nm] ($\Delta\varepsilon$): 311 (62), 290 (−36), 278 (−13); IR: $\tilde{\nu}=2935$w (ν(C−H) aliphatic), 1618s ($\nu_{as}(COO^-)$), 1569m, 1456w, 1423s ($\nu_s(COO^-)$), 1235w, 1092, 1081s (ν(Cl−O)), 862w, 792m, 753m, 622m cm^{-1}; UV/Vis (λ [nm] (ε [M^{-1}cm^{-1}])): 304 (79000), 255 (57000); ES-MS (10^{-4}M in CH_2Cl_2): *m/z*: 1138.91 (100) $[Er_3L_6(OH)]^{2+}$; elemental analysis calcd (%) for $C_{108}H_{109}Er_3N_{12}O_{24}Cl_2{\cdot}3H_2O$: C 50.16, H 4.48, N 6.50; found: C 49.33, H 4.14, N 6.21.

Racemic $[Ln_3\{(\pm)\text{-}L\}_6(OH)(H_2O)_3](ClO_4)_2$ complexes (Ln^{III} = La, Pr, and Eu): These complexes were synthesized according to the same procedure, starting from an artificial racemic mixture of the ligand (±)-HL. The compounds are optical inactive as confirmed by CD and $[\alpha]_D$ measurements. The other analyses (^{1}H NMR, ES-MS, IR, UV) are identical with those of the corresponding enantiopure compounds.

Acknowledgements

This work was supported by the Swiss National Science Foundation (grant no. 2100–068077/200020–105320) and EPFL. We thank Dr. S. Shova and Dr. R. Scopelliti for support with the X-ray measurements and analyses and S. Canarelli and Dr. S. Terenzi for ES mass-spectrometric measurements. M.L. is grateful to Prof. K. Severin for administrative support.

[1] J. A. Peters, J. Huskens, D. J. Raber, *Prog. Nucl. Magn. Reson. Spectrosc.* **1996**, *28*, 283.
[2] D. Bal, W. Gradowska, A. Gryff-Keller, *J. Pharm. Biomed. Anal.* **2002**, *28*, 1061.
[3] S. Masumoto, H. Usuda, M. Suzuki, M. Kanai, M. Shibasaki, *J. Am. Chem. Soc.* **2003**, *125*, 5634.
[4] K. Yabu, S. Masumoto, S. Yamasaki, Y. Hamashima, M. Kanai, W. Du, D. P. Curran, M. Shibasaki, *J. Am. Chem. Soc.* **2001**, *123*, 9908.
[5] K. Mikami, M. Terada, H. Matsuzawa, *Angew. Chem.* **2002**, *114*, 3704; *Angew. Chem. Int. Ed.* **2002**, *41*, 3554; .
[6] J. Inanaga, H. Furuno, T. Hayano, *Chem. Rev.* **2002**, *102*, 2211.
[7] H. G. Brittain, *Coord. Chem. Rev.* **1983**, *48*, 243.
[8] H. G. Brittain, *J. Coord. Chem.* **1989**, *20*, 331.
[9] T. Parac-Vogt, K. Binnemans, C. Görller-Walrand, *ChemPhysChem* **2001**, *2*, 767.
[10] N. Coruh, G. L. Hilmes, J. P. Riehl, *Inorg. Chem.* **1988**, *27*, 3647.
[11] S. Wu, G. L. Hilmes, J. P. Riehl, *J. Phys. Chem.* **1989**, *93*, 2307.
[12] S. C. J. Meskers, H. P. J. M. Dekkers, *J. Phys. Chem. A* **2001**, *105*, 4589.
[13] H. Tsukube, S. Shinoda, *Chem. Rev.* **2002**, *102*, 2389.
[14] H. Tsukube, T. Yamada, S. Shinoda, *J. Alloys Compd.* **2004**, *114*, 3704.
[15] R. S. Dickins, T. Gunnlaugsson, D. Parker, R. D. Peacock, *Chem. Commun.* **1998**, 1643.
[16] H. Tsukube, S. Shinoda, *Enantiomer* **2000**, *5*, 13.
[17] H. G. Brittain, *Inorg. Chem.* **1980**, *19*, 2233.
[18] H. C. Aspinall, *Chem. Rev.* **2002**, *102*, 1807.
[19] D. Parker, *Chem. Soc. Rev.* **2004**, *33*, 156.
[20] J. Gregolinski, J. Lisowski, *Angew. Chem.* **2006**, *118*, 6268; *Angew. Chem. Int. Ed.* **2006**, *45*, 6122.
[21] G. Muller, J.-C. G. Bünzli, J. P. Riehl, D. Suhr, A. von Zelewsky, H. Mürner, *Chem. Commun.* **2002**, 1522.
[22] J. J. Lessmann, W. D. Horrocks, *Inorg. Chem.* **2000**, *39*, 3114.
[23] M. Cantuel, G. Bernardinelli, G. Muller, J. P. Riehl, C. Piguet, *Inorg. Chem.* **2004**, *43*, 1840.
[24] O. Mamula, A. von Zelewsky, *Coord. Chem. Rev.* **2003**, *242*, 87.

[25] M. Lama, O. Mamula, R. Scopelliti, *Synlett* **2004**, *10*, 1808.
[26] O. Mamula, M. Lama, S. Telfer, A. Nakamura, R. Kuroda, H. Stoeckli-Evans, S. R. , *Angew. Chem.* **2005**, *117*, 2583; *Angew. Chem. Int. Ed.* **2005**, *44*, 2527; .
[27] O. Mamula, M. Lama, H. Stoeckli-Evans, S. Shova, *Angew. Chem.* **2006**, *118*, 5062; *Angew. Chem. Int. Ed.* **2006**, *45*, 4940.
[28] P. Hayoz, A. von Zelewsky, *Tetrahedron Lett.* **1992**, *33*, 5165.
[29] W. von Doering, V. Z. Pasternak, *J. Am. Chem. Soc.* **1950**, *72*, 143.
[30] K. Nakamoto, *J. Phys. Chem.* **1960**, *64*, 1420.
[31] O. Mamula, A. von Zelewsky, T. Bark, H. Stoeckli-Evans, A. Neels, G. Bernardinelli, *Chem. Eur. J.* **2000**, *6*, 3575.
[32] M. Düggeli, T. Christen, A. von Zelewsky, *Chem. Eur. J.* **2005**, *11*, 185.
[33] S. T. Howard, *J. Am. Chem. Soc.* **1996**, *118*, 10269.
[34] P. E. Fielding, R. J. W. Le Fèvre, *J. Chem. Soc.* **1951**, 1811.
[35] R. Wietzke, M. Mazzanti, J.-M. Latour, J. Pécaut, *J. Chem. Soc. Dalton Trans.* **1998**, 4087.
[36] D. R. van Staveren, G. R. van Albada, J. G. Haasnoot, H. Kooijman, A. M. Manotti Lanfredi, P. J. Nieuwenhuizen, A. L. Spek, F. Ugozzoli, T. Weyhermuller, J. Reedijk, *Inorg. Chim. Acta* **2001**, *315*, 163.
[37] R. Ziessel, L. J. Charbonniere, M. Cesario, T. Prange, M. Guardigli, A. Roda, A. van Dorsselaer, H. Nierengarten, *Supramol. Chem.* **2003**, *15*, 277.
[38] G. R. Giesbrecht, G. E. Collis, J. C. Gordon, D. L. Clark, B. L. Scott, N. J. Hardman, *J. Organomet. Chem.* **2004**, *689*, 2177.
[39] J. Xu, E. Radkov, M. Ziegler, K. N. Raymond, *Inorg. Chem.* **2000**, *39*, 4156.
[40] J.-C. G. Bünzli, J.-R. Yersin, C. Mabillard, *Inorg. Chem.* **1982**, *21*, 1471.
[41] G. B. Deacon, R. J. Phillips, *Coord. Chem. Rev.* **1980**, *33*, 227.
[42] K. Nakamoto, *Infrared and Raman Spectra of Inorganic and Coordination Compounds*, Wiley-Interscience, New York, **1990**.
[43] P. Krumholz, *J. Am. Chem. Soc.* **1951**, *73*, 3487.
[44] S. Comby, D. Imbert, A.-S. Chauvin, J.-C. G. Bünzli, *Inorg. Chem.* **2006**, *45*, 732.
[45] A. Beeby, I. M. Clarkson, R. S. Dickins, S. Faulkner, D. Parker, L. Royle, A. S. de Sousa, J. A. G. Williams, M. Woods, *Perkin Trans. 2* **1999**, 493.
[46] A. P. Bassett, S. W. Magennis, P. B. Glover, D. J. Lewis, N. spencer, S. Parsons, R. M. Williams, L. De Cola, Z. Pikramenou, *J. Am. Chem. Soc.* **2004**, *126*, 9413.
[47] M. P. Oude Wolbers, F. C. J. M. van Veggel, B. H. M. Snellink-Ruël, J. W. Hofstraat, F. A. J. Geurts, D. N. Reinhoudt, *Perkin Trans. 2* **1998**, 2141.
[48] S. Quici, M. Cavazzini, G. Marzanni, G. Accorsi, N. Armaroli, B. Ventura, F. Barigelletti, *Inorg. Chem.* **2005**, *44*, 529.
[49] M. Ziegler, V. Monney, H. Stoeckli-Evans, A. Von Zelewsky, I. Sasaki, G. Dupic, J.-C. Daran, G. G. A. Balavoine, *J. Chem. Soc. Dalton Trans.* **1999**, 667.
[50] S. Telfer, N. Tajima, R. Kuroda, M. Cantuel, C. Piguet, *Inorg. Chem.* **2004**, *43*, 5302.
[51] S. Telfer, N. Tajima, R. Kuroda, *J. Am. Chem. Soc.* **2004**, *126*, 1408.
[52] A. Rodger, B. Norden, *Circular Dichroism and Linear Dichroism*, Oxford University Press, Oxford, **1997**.
[53] The spectrum of tris(Ln[(+)-L]$_2$) in acetonitrile previously reported and ascribed solely to internuclear exciton coupling (see reference [26]) is different relative to the spectrum recorded in CH_2Cl_2; this behavior is because the trinuclear species undergo structural reorganization in acetonitrile that mainly leads to tetranuclear species (see reference [27]).
[54] F. Richardson, *Inorg. Chem.* **1980**, *19*, 2806.
[55] R. S. Dickins, J. A. K. Howard, C. L. Maupin, J. M. Moloney, D. Parker, J. P. Riehl, G. Siligardi, J. A. G. Williams, *Chem. Eur. J.* **1999**, *5*, 1095.
[56] N. C. Thompson, D. Parker, H. Schmitt-Willich, D. Sülzle, G. Muller, J. P. Riehl, *Dalton Trans.* **2004**, 1892.
[57] R. S. Dickins, J. A. K. Howard, J. M. Moloney, D. Parker, R. D. Peacock, G. Siligardi, *Chem. Commun.* **1997**, 1747.
[58] P. Gawryszewska, J. Legendziewicz, Z. Ciunik, N. Esfandiari, G. Muller, C. Piguet, M. Cantuel, J. P. Riehl, *Chirality* **2006**, *18*, 406.
[59] O. Mamula, A. von Zelewsky, P. Brodard, C.-W. Schläpfer, G. Bernardinelli, H. Stoeckli-Evans, *Chem. Eur. J.* **2005**, *11*, 3049.
[60] A. Wu, L. Isaacs, *J. Am. Chem. Soc.* **2003**, *125*, 4831.
[61] H.-J. Kim, D. Moon, M. S. Lah, J.-I. Hong, *Angew. Chem.* **2002**, *114*, 3306; *Angew. Chem. Int. Ed.* **2002**, *41*, 3174.
[62] E. J. Enenmark, T. D. Stack, *Angew. Chem. Int. Ed.* **1998**, *37*, 932.
[63] M. Albrecht, M. Schneider, H. Röttele, *Angew. Chem.* **1999**, *111*, 512; *Angew. Chem. Int. Ed.* **1999**, *38*, 557.
[64] H.-J. Kim, M. S. Lah, J.-I. Hong, *Chem. Commun.* **2001**, 743.
[65] C. G. Claessens, T. Torres, *J. Am. Chem. Soc.* **2002**, *124*, 14522.
[66] I. Alkorta, J. Elguero, *J. Am. Chem. Soc.* **2002**, *124*, 1488.
[67] J. F. Desreux, in *Lanthanide Probes in Life, Chemical and Earth Sciences. Theory and Practice.* (Eds.: J.-C. G. Bünzli, G. R. Choppin), Elsevier Science, Amsterdam, **1989**.
[68] W. C. Wosley, *J. Chem. Educ.* **1973**, *50*, A335.
[69] K. N. Raymond, *Chem. Eng. News* **1983**, *Dec 12*, 2.
[70] G. M. Sheldrick, *Acta Crystallogr. Sect. A* **1990**, *A46*, 467.
[71] G. M. Sheldrick, Programs for the Determination and Refinement of Crystal Structures, University of Göttingen, Germany, **1997**.
[72] M. Krompiec, L. Patiny, in *Chemcalc*, http://www.chemcalc.org/, **2001**.
[73] A. Juris, V. Balzani, F. Barigelletti, S. Campagna, P. Belser, A. von Zelewsky, *Coord. Chem. Rev.* **1988**, *84*, 85.
[74] W. H. Melhuish, *J. Phys. Chem.* **1961**, *65*, 229.
[75] S. B. Meshkova, Z. B. Topilova, D. V. Bolshoy, S. V. Beltyukova, M. P. Tsvirko, Y. V. Venchikov, V. Ya, *Acta Phys. Pol. A* **1999**, *95*, 983.

Received: February 27, 2007
Published online: July 10, 2007

